Use of Image Registration and Fusion Algorithms and Techniques in Radiotherapy: Report of the AAPM Radiation Therapy Committee Task Group No. 132

Kristy K Brock, Chair
Department of Imaging Physics
The University of Texas MD Anderson Cancer Center
1400 Pressler St
FCT 14.6048
Houston, TX 77030
kkbrock@mdanderson.org

Sasa Mutic
Department of Radiation Oncology, Washington University School of Medicine, St. Louis, Missouri

Todd R McNutt
Department of Radiation Oncology, Johns Hopkins Medical Institute, Baltimore, Maryland

Hua Li
Department of Radiation Oncology, Washington University School of Medicine, St. Louis, Missouri

Marc L Kessler
Department of Radiation Oncology, University of Michigan, Ann Arbor, Michigan

Image registration and fusion algorithms exist in almost every software system that creates or uses images in radiotherapy. Most treatment planning systems support some form of image registration and fusion to allow the use of multimodality and time-series image data and even anatomical atlases to assist in target volume and normal tissue delineation. Treatment delivery systems perform registration and fusion between the planning images and the in-room images acquired during the treatment to assist patient positioning. Advanced applications are beginning to support daily dose assessment and enable adaptive radiotherapy using image registration and fusion to propagate contours and accumulate dose between image data taken over the course of therapy to provide up-to-date estimates of anatomical changes and delivered dose. This information aids in the detection of anatomical and functional changes that might elicit changes in the treatment plan or prescription.

Since the output of the image registration process is always used as the input of another process for planning or delivery, it is important to understand and communicate the uncertainty associated with the software in general and the result of a specific registration. Unfortunately, there is no standard mathematical formalism to perform this for real world situations where noise, distortion, and complex anatomical variations can occur. Validation of the software systems performance is also complicated by the lack of documentation available from commercial systems leading to use of these systems in undesirable 'black-box' fashion.

In view of this situation and the central role that image registration and fusion play in treatment planning and delivery, the Therapy Physics Committee of the American Association of Physicists in Medicine commissioned Task Group 132 to review current approaches and solutions for image registration (both rigid and deformable) in radiotherapy and to provide recommendations for quality assurance and quality control of these clinical processes.

Keywords: image registration, quality assurance, image fusion, adaptive radiotherapy,

TABLE OF CONTENTS

I. INTRODUCTION

a. Image Data in Radiotherapy

The practice of modern radiotherapy involves the quantitative use of several types of image data. Image data from various modalities are used in treatment planning, treatment delivery and treatment monitoring. In the process of treatment planning, X-ray computed tomography (CT) is typically used as the primary imaging modality to construct detailed three dimensional anatomic and physical models of the patient. These models are used to design beam arrangements and shapes, to calculate the dose delivered by these beams and as a guide to position the patient for treatment. Magnetic resonance imaging (MRI) techniques provide exquisite soft tissue contrast for tissue delineation and estimates of physiologic and metabolic information. Nuclear medicine imaging techniques such as positron emission tomography (PET) and single photon emission computed tomography (SPECT) provide dynamic data on physiologic and metabolic process such as glucose metabolism and DNA synthesis.

During the process of treatment delivery, volumetric x-ray imaging technology has been incorporated into the treatment rooms as kilovoltage (kV) and megavoltage (MV) CT imaging systems with fan-beam and cone-beam geometries. Real time volumetric ultrasound (US) can also be used to localize internal anatomy at the time of treatment. Research and development is currently ongoing to enable integration of real-time MR imaging directly with treatment machines. In addition to general set up and target localization, these on-board images can also be used to monitor and track soft tissue changes during therapy and to support plan adaptation.

b. Use of Image Registration and Fusion in Radiotherapy

Image registration is the process of determining the geometric transformation that relates identical (anatomic) points in two image series: a moving dataset (Study A) and a stationary source dataset (Study B). The main uses of image registration and fusion in radiotherapy can be categorized into the following three essential steps.

Image Registration for Segmentation Image registration is often used to segment (manually, semi-automatically, or automatically) target volumes and normal tissues through anatomical atlases or between images of the same patient obtained at different time points (e.g. adaptation).

Image Registration for Multi-Modality or Adaptive Treatment Planning: Image registration and fusion are often used in treatment planning to combine information obtained from different imaging modalities (e.g. MR, PET, SPECT and CT) together for delineation of tumor volumes and/or normal tissues.   Registration is also used to map regions of interest delineations from one imaging study of the patient to another or from a reference set of anatomical contours to a patient specific image. Software systems that support adaptive radiotherapy use image registration and fusion to propagate dose from 3D treatment images back to a reference (planning) geometry, enable detection of anatomic and functional changes that might elicit changes in the treatment plan or prescription, and provide up-to-date estimates of delivered dose.

Image Registration for Image-Guided Radiotherapy: Treatment delivery systems use image registration and fusion between images used for planning and images acquired at the time of treatment to assist with patient positioning. Registration is required to determine the offset of the patient at the time of treatment from the planned position. The transformation determined from the image registration is typically used to perform an adjustment to the patient position.

Image Registration for Response Assessment: The evaluation of treatment response also uses image registration between the images used for treatment planning and those obtained at follow-up. Although registration is not required for simple comparisons of tumor measurements, more advanced assessment, e.g. changes in functional imaging, requires precision in image registration.

The requirements and challenges for timeliness and accuracy vary between the above four main uses. Image registration for planning has relaxed time constraints, as the process typically spans several days. However, image registration at the treatment delivery unit has high demands for timeliness, as the patient is awaiting treatment. This includes registration for treatment delivery and online treatment adaptation. Although high levels of accuracy are expected in all applications, the impact of inaccuracies often depends on the propagation of that error. Registration errors made during treatment planning will impact the entire treatment course, therefore resulting in a high demand for accuracy. Registration errors made at an individual fraction of treatment delivery will likely impact the delivery of that fraction only. For a treatment course with a large number of fractions, the impact of an error at one fraction will be less. Systematic errors in image registration or operator error in the registration process may impact the delivery of all treatment fractions. The

impact of inaccuracies in adaptation depends on the timing of the adaptation and the fraction of the planned dose that will be delivered under the new plan.

c. Clinical Integration of image registration and fusion QA program

This task group recommends implementation of a formal image registration quality assurance (QA) program in individual facilities. The program should be guided and structured based on the recommendations provided here with the considerations described below. The main purpose of the program should be to ensure accuracy and quality of individual patient image registration. The organization and expectations of the program should be formally documented and the roles and responsibilities of individual practitioners in this process should be defined. The program should be managed by the Quality Assurance Committee (QAC). The program considerations should include:

1. Validation and quality assurance of image registration and fusion at treatment planning, treatment delivery, adaptive re-planning, and response assessment
2. Commissioning image registration and fusion software to ensure accuracy of the tools used
3. Define/assign the role of each team member and tailor workflow and tolerances appropriately depending on the intended use of the image registration
4. Clinical verification of image registration for individual patients.

It is intended that these recommendations will be used in conjunction with other recommendations of the AAPM task groups, as indicated in Figure 1.

Details of the clinical implementation of this task group's recommendations can be varied for each specific institution and depend on a broad scope of aspects which include: the individual clinical setting and resources, the purpose of image registration (Section I.b), the timeline for an individual image registration (when a registration is performed in the overall treatment process), the time allotted for image registration (how quickly an image registration needs to be performed and verified), the capabilities of a specific registration software package, etc. Figure 1 shows a typical clinical implementation of image registration process and the possible locations where this and other task group's recommendations are applicable. The figure also shows image registration practices are likely as diverse as any other process in radiotherapy and global recommendations, which are universally applicable to all individual applications, are impractical. The concepts described here provide a general approach and framework which individual facilities should consider to ensure that they perform high quality and safe radiotherapy. However, it is ultimately the responsibility of the individual facilities and their individual QAC to determine the appropriateness of recommendations provided here to their individual use cases and the needs of their image registration program.
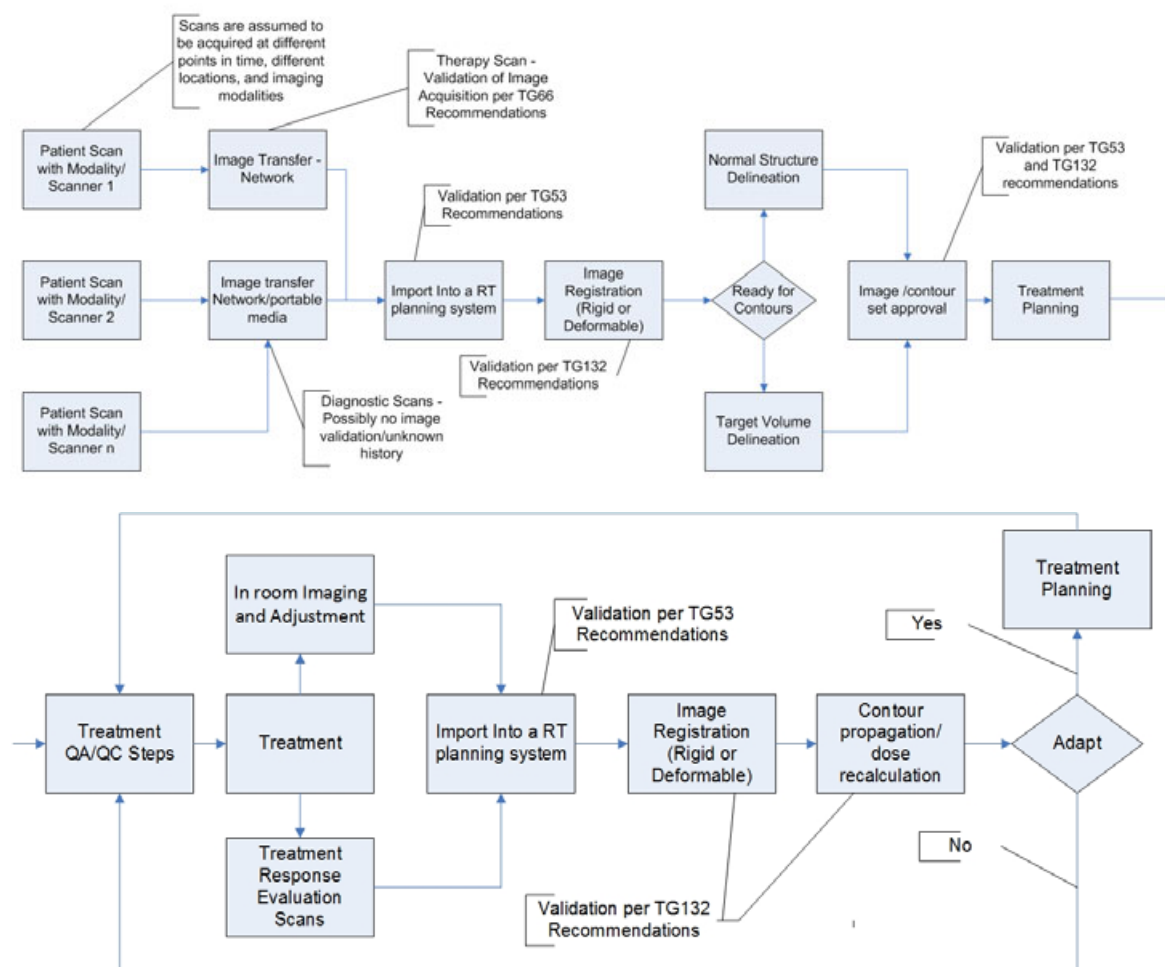
Figure 1. Image data and processing workflow in radiotherapy planning, treatment, and adaptation. Task Groups from the American Association of Physicists in Medicine [TG].

d. Glossary of Terms

Image registration – the process of determining the geometric transformation that relates identical (anatomic) points in two image series: a moving dataset (Study A) and a stationary source dataset (Study B)

Image fusion – the combined display of the mapped data from the moving dataset with the stationary dataset

Transformation – the function that is applied to the moving image (Study A) to align it to the stationary image (Study B)

Registration (or similarity) metric – quantifies the degree to which the pair of imaging studies are aligned

Rigid registration – a registration where the transformation preserves the distance between all points in the image. A rigid registration can include translation in all directions as well as rotations in all directions.

Affine registration – a registration that includes the transformations from rigid registration and adds the additional transformations of scaling, shearing, and plane reflection. The distance between all points is not maintained, as in rigid registration, however parallel lines remain parallel after the transformation.

Deformable registration – a registration transformation can also be spatially variant where the number of degrees of freedom can be as large as three times the number of voxels in the source dataset (e.g., a unique displacement vector for every voxel in the source dataset)

II. Techniques for Image Registration

A brief review of image registration and fusion algorithms is presented here. However, for a comprehensive description the reader is referred to the literature[1-7]. For generalization purposes, the following nomenclature will be used throughout the report: Study A and Study B will refer to any two image sets to be registered in which A is the moving data set (e.g. the dataset that is being transformed or deformed to match another image) while B is the stationary data set (e.g. the dataset that another image is being registered to). It is important to note that these terms are intentionally general as the radiotherapy application will dictate which image is moving and which image is stationary. For example, in radiation therapy treatment planning, if an MR image is to be registered to the CT planning image, the MR image is the moving image and the CT is the stationary image. However, for adaptive radiotherapy, the original planning CT may be the moving image and the mid-treatment CT the stationary image to enable the dose from the original CT to be mapped onto the new CT. Transformation T will refer to the registration matrix (rigid, affine, or deformable; as defined below) that will describe where a point from the moving image maps on the fixed image. A prime symbol will be used to denote the application of the transformation matrix to the image set (e.g. Study A' will indicate the result of applying a transformation T to Study A to create an image that is registered to Study B).

As summarized by Maintz and Viergever[8], registration is defined by 9 criteria:
    A. Dimensionality
    B. Nature of registration basis
    C. Nature of transformation
    D. Domain of transformation
    E. Interaction
    F. Optimization procedure
    G. Modalities involved
    H. Subject
    I. Object

A. Dimensionality

Images in radiotherapy can have a dimensionality of 2D or 3D. For generalization and comprehensiveness, the images are assumed to be 3D; however, the same principles apply for a 2D to 2D registration, only with fewer parameters reflecting only translation in 2 dimensions and rotation in 1 dimension. Due to the inherent limitation in the data, 2D to 2D registration is generally limited to rigid registration in practical applications.

B. Nature of Registration Basis

The nature of the registration basis, whether the registration is extrinsic, e.g. using invasive or non-invasive frames, molds, or fiducials, or intrinsic, using image features or voxel properties can simplify the registration and guide the user to select the best registration metric.

A *registration metric* must be devised which quantifies the degree to which the pair of imaging studies are aligned. Using standard optimization techniques, the transformation parameters are iteratively manipulated until this metric is minimized or maximized, where the minimization or maximization of the metric corresponds to the best alignment of the two images. Most registration approaches in use today can be classified as either *geometry-based* or *intensity-based*. Geometry-based metrics make use of features extracted from the image data such as anatomic or artificial landmarks and organ boundaries while intensity-based metrics use the image voxel data directly.

Geometry or Feature-based Metrics

The most common geometry-based registration metrics involve the use of *point matching* or *surface matching*. For point matching, the coordinates of pairs of corresponding points from Studies *A* and *B* (p_A and p_B in equation 1) are used to define the registration metric. These points can be anatomic landmarks or implanted or externally-placed fiducial markers. The registration metric R is defined as the sum of the squared distances between corresponding points, where N is the total number of points;

$$R= \Sigma \, (p_{A'} - p_B)^2 / \; N. \tag{1}$$

In equation 1, the summation is over the number of matched points or surface points, N, and the division of the summation by N is to normalize the metric. To compute the rotations and translations for a rigid transformation, a minimum of three pairs of points are required. For affine transformations, a minimum of four pairs of non-coplanar points are required.

Alternatively, surface matching does not require a one to one correspondence of specific points but rather tries to maximize the overlap between corresponding surfaces extracted from two image studies, such as the brain or skull surface or pelvic bones. The surfaces from Study *B* are represented as a binary volume or as a polygon surface and the surfaces from Study *A* are represented as a set of points sampled from the surface. The metric, which represents the degree of mismatch between the two datasets, can be computed as the sum or average of the squared distances of closest approach from the points from Study *A* ($p_{A'}$ in equation 2) to the surfaces from Study *B* (S_B), where N is the number of points in Study A. It is written as

$$R = \Sigma \ \text{dist}(p_{A'}, S_B)^2 \ / \ N, \qquad\qquad (2)$$

where dist($p_{A'}$, S_B) computes the (minimum) distance between point $p_{A'}$ and the surfaces S_B. In equation 2, the summation is over the number of points, N, in Study A and the division of the summation by N is to normalize the metric.

As a surface-matching technique, Chamfer matching is statistically similar to correlation; however, it is simplified to improve computational speed. [9-12] In Chamfer matching, the corresponding region in each image is segmented (either automatically, often using thresholding techniques, or manually). The segmentation is then simplified into an image with 0 and 1 values indicating the edge of the segmented region. The optimization is then performed to minimize the distance between the two segmented surfaces.

Intensity-based Metrics

To overcome some of the limitations of using explicit geometric features to register image data, another class of registration metrics has been developed which uses the numerical grayscale information directly to measure how well two studies are registered. These similarity metrics are also referred to as *similarity measures* since they determine the similarity between the distributions of corresponding voxel values from Study B and a transformed version of Study A (e.g. A'). Several mathematical formulations are used to measure this similarity. The more common similarity measures in clinical use include: sum of squared differences, cross correlation, and mutual information.

The *sum of squared differences* (SSD)[13-17] metric is computed as the average squared intensity (I_A and I_B) difference between Study *A* and Study *B*, where N is the number of voxels evaluated.

$$SSD = \Sigma(I_{A'} - I_B)^2 \ / \ N. \qquad\qquad (3)$$

In equation 3, the summation is over the number of voxels evaluated, N, and the division of the summation by N is to normalize the metric. This metric is simple to compute and is effective for registering two imaging studies which have essentially *identical* intensities for corresponding anatomy, such as serial or 4-D CT data.

An alternative technique is the use of the *cross correlation* (C)[18-23] metric, which measures the similarity in the image signal. Rather than minimizing the intensity difference, cross correlation registration maximizes the intensity product, as shown in 4A. The limitation of this metric is that it is sensitive to the changes in the voxel value (increases in the intensity values of one image increases the cross correlation).

$$C = \sum_{\vec{x}} B(\vec{x}) \cdot T\big(A(\vec{x})\big) \qquad\qquad (4A)$$

To overcome these limitations, the normalized version of the cross correlation metric (*correlation coefficient*) can be used, which is shown in equation 4B. The assumption in the correlation coefficient is that there is a linear relationship between the intensity values in each image, therefore, this metric can handle differences in image contrast and brightness in the image.

$$CC = \frac{\sum_{\vec{x}}(A(\vec{x})-\bar{A})(T(B(\vec{x}))-\bar{B})}{\sqrt{\sum_{\vec{x}}(A(\vec{x})-\bar{A})^2 \sum_{\vec{x}}(T(B(\vec{x}))-\bar{B})^2}} \qquad (4B)$$

For data from different modalities where the pixel intensities of corresponding anatomy are typically (and inherently) different, registration metrics based on simple differences or products of intensities are not effective. In these cases, sophisticated metrics based on intensity statistics are more appropriate. When using these metrics, there is no dependence on the *absolute* intensity values. One such metric that has proven very effective for registering image data from different modalities is called *mutual information* (MI)[24-43]. Mutual information seeks to align voxels whose values have common probabilities of being present in their respective image sets. In equation 5, the summation is over the intensity levels in image A' ($I_{A'}$) and Image B (I_B), where $p(I_{A'})$ and $p(I_B)$ are the probability distribution functions of the intensities $I_{A'}$ and I_B, respectively and $p(I_{A'}, I_B)$ is the joint probability distribution function.

$$MI(I_{A'}, I_B) = \sum_B \sum_A p(I_{A'}, I_B) \log_2[p(I_{A'}, I_B)/p(I_{A'})p(I_B)] \qquad (5)$$

Commonly used similarity metrics are listed in Table 1.

Table 1. Similarity Metrics

Class	Metric	Description
Voxel Intensity-based	Sum of the squared difference (SSD) (Mean squared difference, MSD)	Assumes an equivalent relationship between voxel intensities in 2 images, single modality
	Correlation coefficient (CC)	Assumes linear relationship between voxel intensities in 2 images, single modality or possibly small region of multi-modality
	Mutual Information (MI)	Assumes statistical relationship between voxel intensities in 2 images, single or multi-modality
Feature-based	Point-based	Assumes direct relationship between points identified on 2 images, single or multi-modality
	Contour-based	Assumes direct relationship of identified boundaries of regions of interest in 2 images, single or multi-modality

C. Nature of Transformation

Image registration algorithms require four components: a geometric transformation T, a registration metric (described above in B), an optimizer (described below in F) which drives the algorithm to find the best result of the registration metric such as maximization of mutual information between A' and B, as illustrated in Figure 2, and finally image resampling and application of the transformation.
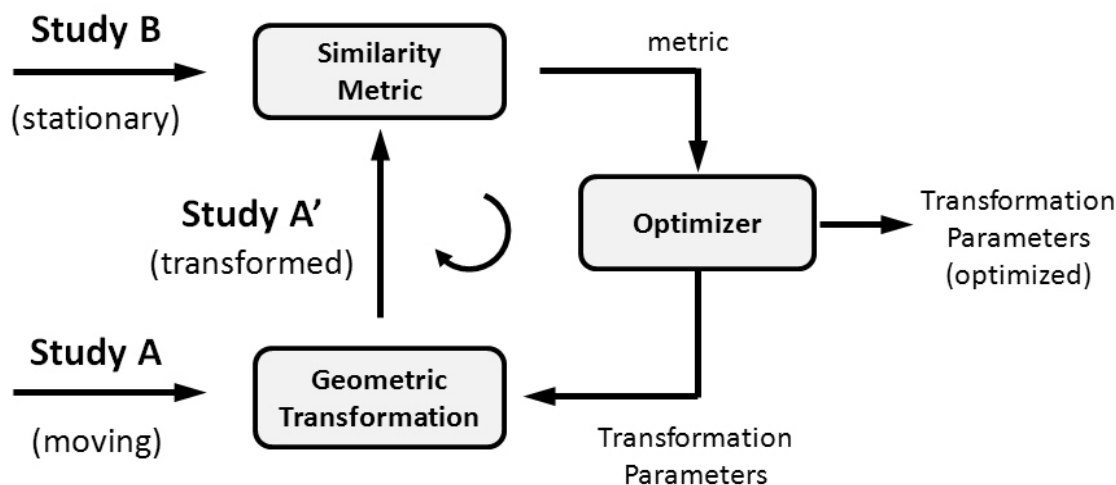

Figure 2. Basic mechanics of image registration algorithms

The fundamental task of image registration is to find the transformation T. The transformation T is applied to the moving image (Study A) to align it to the stationary image (Study B). In general, this transformation can be written as

$$\mathbf{X}_B = T(\mathbf{X}_A, \{\beta\}) \tag{6}$$

where X_A is the coordinate of the point in the moving dataset A, X_B is the coordinate of the same anatomic point in the stationary dataset B, and $\{\beta\}$ is the set of parameters of the transformation. The output of the image registration process is the parameters $\{\beta\}$ for a particular pair of imaging studies (Figure 2). The number of the parameters required to determine the transformation depends on the form of T, which in turn depends on the anatomical site, clinical application, and the imaging modalities involved. The transformation T can be simple, representing a rigid body, consisting of three translation and three rotation parameters (referred to as rigid registration). This can be expanded to nine or twelve parameters to account for affine transformation (e.g. accounting for scaling, shearing, and plane reflection). The transformation can also be spatially variant where the number of degrees of freedom can be as large as three times the number of voxels in the source dataset (e.g., a unique displacement vector for every voxel in the source dataset), referred to as deformable registration. Typically, these spatially variant vector fields are constrained by a regularization function to ensure that they represent an anatomical and physiologically realistic

transformation. A regularization function is used to restrict unrealistic motion and to generate a smooth deformation field (i.e. classifying a region as bone and restricting the degree of deformation in this region). Commonly used image registration transformation algorithms are listed in Table 2, organized by class of transformation: those that have a physical basis for the transformation and those that are a geometric construct. The registration matrix resulting from a deformable registration is often referred to as a deformation vector field, since there can be a unique 3D transformation for each image voxel.

Ideally the transformation T is invertible, but that is not always the case in complex cases (tissue that is only present in 1 of the images) or for transformations that are not well behaved (e.g. the transformation is significantly different when mapping A to B and B to A). Therefore, the user must consider the purpose of the registration and how the transformation will be used to determine which direction the transformation should be generated.

Table 2. Commonly used transformation models. (N = number of voxels in an image)

Class	Transformation	Maximum Dimensionality of Transformation	Description
Geometric	Rigid	6	Allows translation in 3 directions and rotations about 3 axes
	Affine	12	In addition to translation/rotation, allows uniform scaling and sheer (e.g. parallel lines stay parallel)[44-48]
	Free-Form	3N	Local, voxel-based deformation, often regularized by a smoothing parameter
	Global Spline-based methods (e.g. Thin Plate Splines)	3N	Parameterizes deformation using a parametric grid of basis function control points with constrained global influence (e.g. deformation is **global**)[34,49-66]
	Local Spline based methods (.e.g. B-Spline)	3N	Parameterizes deformation using a weighted grid of control points of basis functions with local influence (e.g. deformation is **local**) [17,67-101]

Physical	Viscous/elastic/optical flow (e.g. Demons)	3N	Spatially variant voxel displacement voxel displacement by a vector field in a deforming medium, by intensity gradients (deformation is local) [102-110]
	Finite element methods (FEM)	3N	Spatially variant voxel displacement voxel displacements governed by biomechanical tissue properties (deformation is local) [55,92,111-135]

E. Interaction

It is prudent to acknowledge the role of the user in image registration. The registration can be interactive, semi-automatic, or completely automated. Image registration can be, and has been for many years, performed either completely manually or with manual intervention. The role of the user may be to provide an initial registration when two images have a substantial (i.e. several cm) shift or to adjust the output of the image registration when the user does not feel that an optimal solution has been found. The manual adjustment of the registration following automated registration should be restricted to rigid registration. The direct, unguided manual adjustment of a deformation vector field is not recommended and could lead to erroneous results that are not obvious, however iterative refinement or principled adjustment may aid in achieving a realistic and more accurate registration.

F. Optimization procedure

A myriad of optimization methods are used in rigid and deformable registration algorithms[136-146]. The goal of the optimization is to find the best set of parameters of the transformation to obtain the best image alignment given by the similarity metric. For image based similarity metrics most optimizers are iterative in nature and will repeatedly try different transformation parameters until the resulting value of the similarity metric converges to an optimal value. The primary goal of the optimizer is to be efficient by intelligently finding search directions through the parameter space while also searching the entire parameter space to find the most accurate solutions. Several algorithms are used from gradient based methods that employ the gradient of the similarity metric with respect to the transformation parameters to best choose search directions to more stochastic methods that randomly sample the search space in a controlled fashion. Another important attribute of the optimizer is in how it manages parameter constraints. For example, in deformable image registration, a smoothness constraint may be applied to ensure that a deformation map does not contain any high frequency deformations that are unrealistic. To do this, the transformation parameters themselves will be constrained, and the optimizer has to be able to handle these constraints without generating instabilities in the overall optimization process. Several such considerations are important to the optimization and are dependent on the type of transformation and parameter constraints being used. It is important to understand the optimization approach used by your clinical solution to better appreciate how it converges and where it may have pitfalls.

G. Modalities involved

Image registration for radiotherapy applications often involves several different imaging modalities including CT, PET, SPECT, MR, ultrasound, CBCT, an MVCT. Image registration can therefore be between 2 images of the same modality or between images of different modalities.

H. Subject

Image registration can also be performed between images of the same subject, between images of different subjects, or between an atlas and an individual patient. Image registration between images of the same subject is most common in radiotherapy, however between images of different subjects can be useful to characterize disease or motion across a population. Registration between patient images and an atlas can also be performed for segmentation purposes.

I. Limitations and Challenges

Restricting the registration of two images to simple rigid transformations is often met with remaining uncertainties due to the deformable nature of soft tissue. However, at the present time, the majority of radiotherapy clinics are limited to rigid registration at treatment planning and delivery. In these cases, the user should make tradeoffs to optimize the registration in a way that reduces the uncertainties in the most important regions for the task and account for the uncertainties as appropriate for the clinical care.

Even when deformable registration is available for use, limitations and challenges remain. Regardless of which algorithm is chosen, deformable registration is ill-defined and over-constrained. All algorithms use a model to describe the deformation and as a result will have limitations. For example, many deformable registration algorithms assume smoothness of the vector field. This expectation will lead to registration error when singularity of the vector field exists, such as when registering an open mouth to a closed mouth, an image with a vaginal applicator to one without, or when registering two images where a structure is present in one and not in the other. The large numbers of degrees of freedom in deformable registration may lead to ambiguity in the deformation vector field for some algorithms, such as areas with very low tissue contrast and registration in these areas can be prone to inaccuracies.[147,148]

III. CLINICAL ISSUES AND APPLICATIONS OF IMAGE REGISTRATION IN RADIOTHERAPY

a. Sources of Error due to Data Acquisition

The extent, scan parameters, and the quality of individual imaging studies can affect the accuracy of their registration with other studies.
- **Extent**: A potential complication exists when the physical extent of two studies to be registered are significantly different, leading to limited volumes available for registration and evaluation of its accuracy. The limited extents are typically in patient's cranio-caudal direction, where one study is shorter than the other, but with MR acquisitions, the limited extent can be in all directions, particularly with non-axial plane acquisitions.

- **Scan Parameters**: Scan parameters of the registered imaging studies affect the integrity (sampling/resampling effects) and the size of their voxels (resolution). The voxel integrity can be a problem with MR studies where images acquired in oblique volumes with rectangular voxels need to be significantly manipulated and resampled to match the axial orientation of the CT study. Spatial resolution of PET images can be lower than that of CT or MR studies and can lead to significant resizing and resampling which in turn can affect the values of reconstructed voxels.
- **Quality**: Images of some registered studies can be noisy and of poor quality (by design, e.g. to limit dose, or due to confounding factors, e.g. motion during scanning) leading to a difference in the appearance of images being registered.

The above examples demonstrate the natural variability and possible alterations of imaging studies being registered. Due to the potential and unpredictability of imaging data, it is important to evaluate the appearance of registered studies as well as the registration accuracy for each individual registration. Solutions to address these issues will vary based on extent of the image alteration, options available in the registration system, and the subsequent use of the registered image.

b. Sources of Error in Registration

The process of registration can introduce uncertainties, so it is therefore important that quality assurance and quality control techniques are designed to understand, evaluate, reduce, and account for these uncertainties. Sources of error can generally be divided into input, algorithm, and output.

Uncertainties in the images, the input to the registration, can cause error in the image registration. Artifacts are a common source of uncertainties in images. Image artifacts can be due to the anatomy (such as dental fillings or stents) or motion (e.g. breathing, peristalsis, heartbeat). These image artifacts limit the geometric fidelity of the image by presenting inconsistent anatomy and can lead to errors in the registration. Artifacts in the image due to acquisition (e.g. MR distortion, lack of calibration of the imaging equipment) can also cause errors in the registration. Care should be taken to calibrate the imaging equipment, select the most optimal imaging parameters for acquisition, and avoid anatomy-based artifacts. Other information in the images that are not artifacts can be a source of error, such as large changes in the anatomy between images (e.g. response to therapy or weight loss). Large changes in the tissue especially in areas that lack information (e.g. features and contrast variation) can be especially prone to errors in the registration.

The image registration algorithm can also be a source of error. Optimal selection of the main algorithm components, e.g. similarity metric, transformation model, and optimizer, can aid in mitigating these errors. Using too many or too few degrees of freedom can cause errors in the algorithm. Poorly designed optimizers can result in the algorithm finding a solution in local minima instead of the global minima. Uncertainties in the selection of features or the manual contouring of structures that drive the registration can also be a source of error. Limitations in the model used for the registration can cause errors, such as the inability to handle tissue interfaces that are sliding (e.g. the lung sliding along the rib cage) or tissue loss or gain (e.g. weight loss/gain or tumor response). Models with limited capabilities can introduce error when registering images that show complex changes.

Finally, the use of the registration, the output, can be a source of error. Incorrect interpolation of the registration results can cause error as well as improper extrapolation of the registration field of view. Invalid use of the registration results can also be a source of error for downstream processes, such as contour propagation, dose accumulation, or image guidance.

c. Image Registration for Segmentation

One motivation for registering imaging studies is to be able to map information derived from one study to another (e.g. for image segmentation) or to directly combine or *fuse* the imaging data from the studies to create displays that contain relevant features from each modality. For example, a references image, with all relevant anatomy, can be registered to a patient specific image, and the contours can then be copied onto the patient specific image. In another example, a tumor volume more clearly visualized using MR can be fused with the CT used for treatment planning. If the geometric transformation between the MR study and the treatment planning CT study is known, the clinician is able to outline the tumor on the MR and map these outlines to the CT for planning. This process is called *structure mapping* and is illustrated in Figure 3. This process can also be performed between two images for the purposes of propagating the set of contours on one image to the other image.

If the registration involves rotation and translation, the contours from the secondary image cannot be directly overlaid onto the primary as the image slices do not align. A surface representation of the target volume can be constructed by tessellating or "tiling" the 2-D outlines. Using the computed transformation, the vertices of the surface are mapped from the coordinate system of the secondary image to the coordinate system of the primary image. The transformed surface can be inserted along the image planes of the primary study. The result is a set of outlines of the secondary image defined structure that can be displayed over the primary images. These *derived* outlines can be used in the same manner as other outlines drawn directly on the primary images.
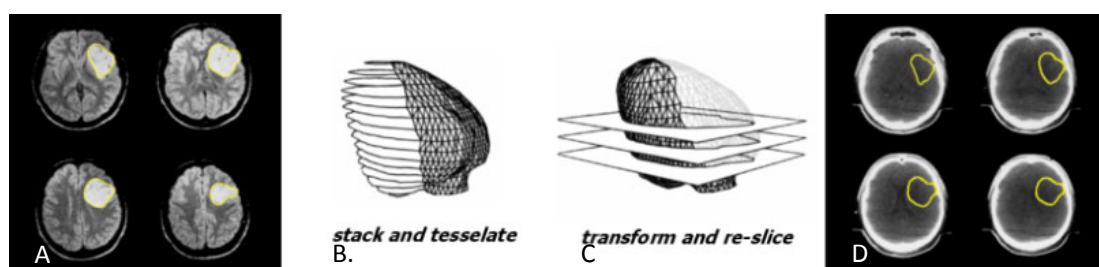

Figure 3. Structure Mapping. A) Tumor volume outlined on a secondary image (e.g. MR in this case). B) Outlines stacked and tessellated to create a surface representation.[149] C) The MR-based surface is mapped to the CT coordinate system and re-sliced along the image planes of the CT study. D) The derived contours are displayed over the CT images.

The goal of the reformatting and interpolation is to create a version of Study A (Study A'') with images that match the size, location and orientation of those in Study B. The voxel values for Study A'' are determined by transforming the coordinates of each voxel in Study *A* using the appropriate registration transformation (producing Study A') and interpolating between the surrounding voxels and reformatting to match Study B (producing Study A''). The result is a set of images from the two studies with the same *effective* scan geometry. These corresponding images can then be combined or fused in various ways to help elucidate the relationship between the data from the two studies or enable delineation of anatomy on the fused images, including the use of overlays, pseudo-coloring, and modified grayscales. For example, functional information from a PET imaging study can be merged or *fused* with the anatomic information from an MR imaging study and displayed as a colorwash overlay.

In addition, 3D dose distributions computed in the coordinate system of one imaging study can be mapped to another (e.g. doses computed on the treatment planning CT can be displayed on an MR).

d. Image Registration for Multi-Modality or Adaptive Treatment Planning

Image registration is necessary when integrating multi-modality images (e.g. CT, MR, PET, and/or CBCT) into treatment planning and plan delivery. The necessary output of this registration is a transformed image that is in the same geometric position as the reference image. The use of multi-instance imaging (e.g. inhale and exhale CT) may also require registration to obtain the motion and/or deformation that is exhibited by the tumor and surrounding critical structures for incorporation into the planning process and dose calculation. In this case, it is the transformation, rather than the transformed image, that is needed.

The complexity of the multi-modality image registration depends on the complexity of the variations in anatomy, including motion and anatomical changes, between the imaging sessions or acquisitions. In some instances, the imaging hardware can be joined (i.e. a PET-CT scanner, SPECT-CT, or PET-MR).This does not guarantee perfect alignment, however, as physiological processes (bladder filling, breathing, peristalsis, etc.) occur between the acquisitions, as well as the possibility of small patient movements.

When the imaging hardware is not combined, some of this complexity can be reduced in multi-modality imaging by taking steps to maintain the same patient configuration between imaging sessions (i.e. use the same immobilization device, minimize the time interval between the acquisition of the images to reduce certain physiological motions such as bladder and stomach filling). By taking these steps, it may be possible to use a simple image registration technique (e.g. rigid registration or rigid registration on a limited field of view) to achieve an acceptable accuracy. However, some issues cannot be addressed through imaging protocols, such as the soft tissue deformation that occurs due to breathing motion, internal organ distortion, and dramatic patient weight loss from planning to plan delivery, where, deformable image registration may be required to achieve the desired level of accuracy. [150]

In addition, image registration is a useful tool to assist with adaptive re-planning, where anatomical changes that are observed over the course of treatment require a modification to the treatment plan to maintain the targeted therapeutic intent and the normal tissue sparing. The complexity that exists between the initial planning images and the image acquired for adaptive replanning cannot be resolved by consistent immobilization as it is the shape, size, and position of the anatomy that has changed. Deformable registration provides the ability to account for these changes and link these two instances of the patient together.

e. Image Registration for Image-Guided Radiotherapy (IGRT)

Image registration for IGRT is performed primarily to guide patient positioning for individual treatment fractions. Therefore, the necessary output of the registration, whether the registration is simple (e.g. rigid) or complex (e.g. deformable), is a numerical transformation that will best align the patient at the time of treatment to the representation of the patient at the time of planning with respect to the treatment isocenter. The resulting transformed image may also be used in image fusion for verification of the registration.

In addition, complex anatomical changes may occur between planning and the treatment fraction, including changes in the physiological state (e.g. bladder/stomach filling), changes in the gross patient position (e.g. neck flexion), or response of the tumor or normal tissue to treatment (e.g. tumor volume reduction). The identification of these changes can be facilitated through image fusion at the treatment fraction.

Both the measurement and the implementation of the measured correction are governed by the system and tools clinically available. Some IGRT-based registration systems allow for the measurement of patient rotation in either one or all three imaging planes. It is important to note that the measured rotation is impacted by the selection of the point of rotation. The influence that the user has on the location of this point is determined by the design of the algorithm and should be investigated by the user prior to using these tools. With advanced treatment hardware, such as a 6 DOF couch, the measured rotations can then be corrected for by rotating the couch. However, if a 6 DOF couch is not available, the user can choose between rotating the table to correct for 1 rotational DOF, which is typically possible with most standard equipment, or the user should determine how to best account for the rotations with only a 3 DOF translation. Murphy provided an excellent technical comment addressing this issue, which the reader is referred to for further information. [151]

f. Image Registration for Response Assessment

The use of image registration to improve the assessment of disease response is an active area of research at the time of this report. Image registration for response assessment can be performed during or following the completion of radiation therapy. It is performed between images of the same or different imaging modalities and the goals often differ from those for treatment planning or guidance. As the name indicates, the registration is performed to enable qualitative or quantitative evaluation of the response of the tumor or normal tissue to radiation. Standard response metrics, such as Response Evaluation Criteria in Solid Tumors (RECIST)[152], perform simple 2D measurements

of the tumor in its largest dimension. While these techniques are simple and do not require registration, they also do not incorporate the heterogeous and complex response of tumors following irradiation. Response assessment in radiotherapy often requires a comparison of functional imaging or analysis of soft tissue imaging beyond the RECIST criteria, which requires image registration. These cases challenge image registration algorithms due to changes in the volume and mass of the tissue of interest as well as large deformation in tissues. When deformable registration is performed between two longitudinal images, the magnitude of response can be evaluated from the deformation vector field. In addition, the complexity of the tumor and normal tissue response can also be characterized by the deformation[153,154].

IV. METHODS FOR VALIDATION AND QUALITY ASSURANCE

a. General Concepts

It is important to clearly identify the terminology used to describe the assurance of quality image registration. The following definitions will be used for this task group report, consistent with the formal US Food and Drug Administration (FDA) definitions.

> ***Validation*** refers to the evaluation of the overall process and toolset to ensure that accurate image registration can be performed on a consistent basis for the intended use (e.g. contouring, image guidance, etc.).

> ***Verification*** is the process of confirming that the accuracy of a specific image registration is acceptable for the intended use (e.g. is the registration of the patient's MR and CT accurate).

> ***Quality Assurance*** is the procedures and process followed to ensure maintenance of quality in each image registration.

Image registration errors can stem from multiple factors such as image distortions, inability to reproducibly select fiducial points represented in both image sets to be registered, registration algorithm limitations, incorrect selection of registration algorithm parameters, etc. The ability to accurately assess registration errors partially depends on the tools provided in the image registration software and the ability of the user to interact with the registration results. Other considerations include spatial distortions (e.g. MR distortion) as well as the final clinical endpoint for evaluated images. The overall image registration accuracy for the majority of clinical applications, where an in-plane resolution is ~1 mm and slice thickness is ~2-3 mm, is typically desired to be within 2 mm. Therefore, the registration evaluation process has to be able to support this accuracy and evaluation tools need to be able to detect registration errors in individual directions that are smaller than the composite error.

The tools needed for registration validation and verification depend on the evaluation method. Software packages used for image registration in radiotherapy should support the methods described in section IV. Independent validation of an application requires access to the geometric transformation. To facilitate this, the software should allow access to and export of the registration matrix or deformation vector field following registration. This export should ideally be in Digital Imaging and Communication in Medicine (DICOM) format, but at minimum in a well-described, easily accessible format. The choice of evaluation method used for validation and verification depends on the specific use of registered images as well as on the registered imaging modalities.

While the registration should be ultimately approved by a trained member of the radiotherapy team prior to use of images, data integrity (i.e. the validity of the interpretation of the image data into a visual image) and registration verification should be performed during each step of image processing and registration and should be the responsibility of the entire radiotherapy team. The scope of the verification tests will depend on the registered imaging modalities, capabilities of the registration system, and the clinical purpose of image registration. The achievable accuracy also depends on the images being registered, their associated voxel size, the degrees of freedom of the registration algorithm, and of course, the amount of deformation between the two images.

b. Qualitative Validation and Verification of Image Registration Accuracy

For initial commissioning of an image registration system, quantitative validation is required; however, for patient specific evaluation of image registration, quantitative verification is not always possible due to limited time and resources and difficulty in determining the ground truth. In routine clinical practice, qualitative verification of image registration should be performed to ensure acceptability of the registration. Common techniques used to enable qualitative evaluation are described and illustrated below in Figure 5. These techniques often rely on the visualization of image fusion.

Once the optimal transformation between a stationary source and moving target dataset is determined (through the identification of the maximum value of the similarity metric), data from the moving dataset can be mapped to the stationary dataset and combined or displayed on or with the stationary dataset. This process is called fusion. An example is shown in Figure 4.
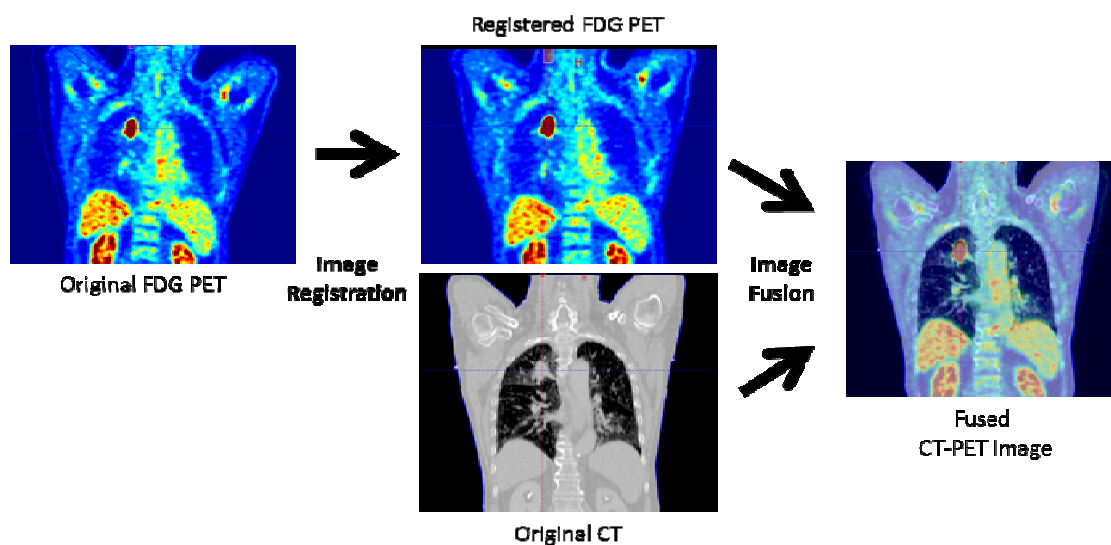

Figure 4. An FDG PET image and a CT image, originally not aligned, underwent image registration (center) and image fusion (right).

These displays allow the individual to select the color mapping, window and level and color blending methods that best visualize the fused image sets. The appropriate use of window/level in both images is critical for these assessments, using different levels to visualize different aspects of the anatomy. Inadequate display settings can blind the user to otherwise obvious errors in registration. Appendix A provides a table with site-based guidance of anatomical structures to use for validation of registration.
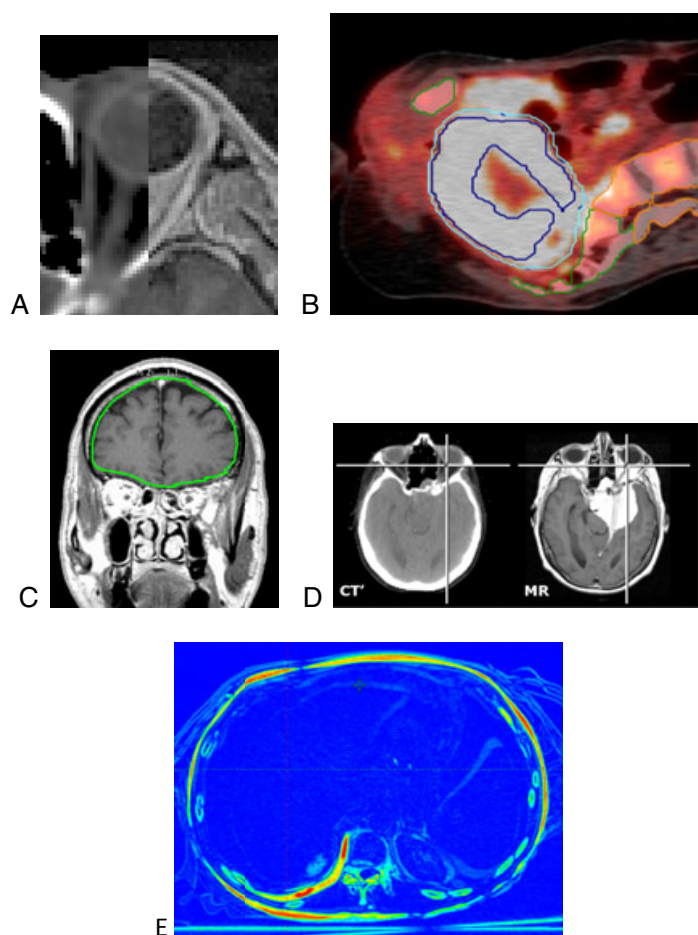
Figure 5.A) Image-image visual validation using split screen displays of native MR and reformatted CT study. B) Region of Interest delineation overlaid on a fused PET and CT. Contoured are target volumes as identified on PET image and pelvic and vertebral bones as delineated on CT images. C) Image-geometry visual validation structure overlay of CT defined brain outlines over MR images. D) Side-by-side display with linked cursor. E) Difference image showing good registration (e.g. solid blue) within the liver, the area of interest, and more uncertainty in the bone and surface (e.g. yellow, green, red color).

Split Screen and Checkerboard Displays

Split screen, floating window (i.e. a window on Study B that shows Study A'), and checkerboard displays as shown in Figure 5.A are the most commonly-used form of qualitative visualization tool for detecting registration error in the clinical setting. They are particularly effective in identifying mismatches between corresponding structures at high contrast tissue interfaces. The split screen partition and checkerboard locations are typically a user-controllable aspect of these displays.[155]

Image Overlay Displays

Image overlay displays as shown in Figure 5.B produce images that are the blended composition of registered images. Often the reference image is presented in gray scale color map and the floating image is presented in a color scale. The user is typically able to control the choice of grayscale and color maps and the fraction of reference and floating image in the blended display.

Difference Image Displays

Difference image displays are useful for intra-modality visualization of registration accuracy (*e.g.,* CT/CT, MR/MR). The display is created by subtraction of co-registered voxel intensities. If the absolute value of the difference is used, a perfect intensity match at the voxel level leads to a display level of 0 (black); as the mismatch gets worse, the color displayed for the voxel gets brighter, approaching white. The utility of these displays in the clinical setting is limited as they are very sensitive to the exact voxel values of the registered datasets.

Contour/structure mapping displays

Contour overlays as shown in Figure 5.B and 5.C are useful for multi-modality image registration. Anatomical contours defined on one imaging modality can then be overlaid, in the same spatial location, on the second imaging modality. Qualitative assessment of correlation of the contour to the anatomy on the secondary image can aid in validating the registration results, although this must be interpreted in the context of the visibility of the anatomy. [156,157]

c. Quantitative Measures of Image Registration Accuracy

Target Registration Error

The alignment of anatomical points is a simple and direct way to quantify the accuracy of registration at a specific location. Increasing the number of points improves the validity of the verification for the overall image registration. The technique is simple in theory, a set of landmarks for corresponding anatomic points are identified on Studies *A* and *B* and the distance between the actual location of the points defined on Study *B* and the resulting transformed locations of the points from Study *A'* is computed. This is often referred to as the target registration error (TRE), which is the average residual error between the identified points on Study B and the points identified on Study A, mapped onto Study A' through image registration.[158] A 'perfect' registration at the location

of the landmark would result in the landmark being in the exact same spatial location in both Study A' and Study B, resulting in a TRE of 0. In practice, it may be difficult to accurately and sufficiently define the appropriate corresponding points, especially when registering multimodality data. There will always be some degree of uncertainty in the location of the corresponding landmarks identified in each image, resulting in a non-zero distance between the landmark identified on Study A and Study B', even after the highest quality image registration. Studies have shown that the uncertainty in point selection is typically less than the voxel size.[34,116] Also, if deformations are involved, the evaluation is not valid for regions away from the defined points.

Mean Distance to Agreement and Dice Similarity Coefficient

The alignment of anatomy or features (e.g. stents) delineated on Study B overlaid onto Study A' can provide a qualitative assessment of the accuracy of registration. By contouring the same structure on Study A', a quantitative assessment of the accuracy can be obtained. Under perfect registration (and perfect delineation) the contour of the anatomy on Study B should perfectly match the contour on Study A'. In practice, they will not perfectly match due to contour variation. Contour variation depends on the imaging modality and structure of interest. For example, Persson et.al. quantified the inter-observer delineation variation to be 2.6 mm for SBRT of peripheral lung tumors using a cross-sectional study design [159], while Brouwer et al. reported a 3D variation about 3.9 mm in delineation of glottis larynx from head-and-neck cancer patients[160]. Inter-observer variation is typically larger than intra-observer variability[159-161], so when evaluating the accuracy of a registration, having the same observer contour the structure on both images will reduce the uncertainty in the metric.

However, the discrepancy between the contours should be within the variation of the observer contouring. Quantitative comparison between the contours can be performed using multiple metrics. Two commonly used approaches are the Dice similarity coefficient (DSC)[162] and mean distance to agreement (MDA)[163], also referred to as the mean distance to conformity. DSC is defined as two times the volume where the two contours overlap divided by the total volume of both contours combined. As the contours approach agreement, the DSC value approaches 1; as the volumes diverge into 2 non-overlapping structures, the DSC value goes to 0. At the time of publication, the calculation of DSC in commercially available registration systems is not standard, although its inclusion in commercial software is a recommendation of this report. However, it is often possible for the user to calculate this using Boolean operators typically available. Given a structure image B (struct_B), the same structure contoured on image A (struc_A), and the mapping of struct_A onto Image B through image registration (resulting in image A' and struct_A' both in the geometrically registered space of Image B) the DSC could be computed as follows: 2*(struct_A' AND struct_B)/(struct_A' OR struct_B). To compute the mean distance to agreement, contour B would be converted into a series of points and the distance of each point to contour A' would be computed. Contour A' would then be converted into points and the distance of each point to contour B would be computed. The average of all distances would then result in the mean distance to agreement. As with DSC, MDA is not a standard feature in commercial registration, but recommended for inclusion. Using the same structure definition described for DSC, the user can estimate the MDA by manually measuring distances between struct_A' and struct_B and calculating the average of these differences.

Jacobian Determinant

Mathematical functions are less commonly used to quantitatively evaluate image registration, often because their interpretation is less clear. The Jacobian determinant can be calculated following a deformable registration between two images and evaluated. The Jacobian determinant identifies the local volume change as a result of the registration. Jacobian determinants greater than 1 indicate volume expansion, between 0 and 1 indicate volume reduction, a value of 1 indicates no change, and a value of less than or equal to 0 indicates non-physical motion (e.g. regions of the image folded onto itself). A Jacobian determinant of less than or equal to zero clearly indicates an erroneous physical modeling of the patient and may indicate an error in the registration or a limitation in the algorithm to handle complex deformation. Any negative values indicate an error in the registration and these areas should be carefully evaluated for their influence on the results and further applications of the registration. However, some volume expansion and contraction is expected in some registrations (e.g. registering an inhale to exhale lung). Large local changes in the Jacobian determinant could also indicate a registration error (e.g. voxels in a small 2x2 region with a Jacobian of 10 while surrounding voxels have a Jacobian of 1).

Additionally, the metrics used to drive registration (i.e. SSD, CC, and MI) can also be used to assess the registration as long as the metric was not used in the registration algorithm itself. These metrics can be easily and efficiently employed to assess the registration. However, it is difficult to convert these metrics into quantitative measures of spatial accuracy.

Consistency

In addition, quantitative metrics of consistency can be performed. These do not provide direct verification, but do provide evidence of a stable and well understood system. These techniques include performing the registration in both directions to ensure that the registration is inverse consistent, i.e. registering A to B and then B to A. The registration should be consistent in magnitude but opposite in direction. When multiple images are to be registered, transitivity can be measured by performing the registration of A to B and combining this with the registration results of B to C. This combined registration result should be the same as the registration of A to C.

The quantitative metrics are summarized in Table 3. As with the qualitative metrics, the tolerance listed is the target tolerance for the registration. The multi-disciplinary team, including the physicist and physician, should evaluate if additional uncertainty beyond the tolerance should be added to the uncertainty margin for the patient. This will depend on the clinical protocol. Tolerances listed are also for standard treatment, stereotactic radiosurgery tolerances are 1 mm, corresponding to the smaller voxel dimension.

Table 3. Quantitative Metrics to Evaluate Image Registration

Technique	Evaluation Metric	Tolerance
Target Registration Error (TRE)	Point-based accuracy metric using implanted or naturally occurring landmarks visualized on a pair of images	Maximum voxel dimension (~2-3 mm)
Mean Distance to Agreement (MDA)	Mean surface distance between 2 contours on registered images	Within the contouring uncertainty of the structure or maximum voxel dimension (~2-3 mm)
Dice Similarity Coefficient (DSC)	Volumetric overlap of 2 contours on registered images	Within the contouring uncertainty of the structure (~0.80-0.90*)
Jacobian Determinant	Volume expansion or contraction resulting from a deformable image registration	No negative values, values deviating from 1 as expected from clinical scenario (0-1 for structures expected to reduce in volume, greater than 1 for structures expected to expand in volume)
Consistency	Independence of an algorithm to the direction of the registration (image A to image B or image B to image A)	Maximum voxel dimension (~2-3 mm)

*DSC calculations are dependent on the volume of the structure, therefore very large or very small structures may have different expected DSC values for contour uncertainty.

d. Specific Considerations of Phantoms

During commissioning of an image registration system, phantoms can also be very useful to quantitatively assess the accuracy of image registration. Phantoms can be physical (tangible objects and their images can be acquired on various scanners) or virtual (digital). For physical phantoms, the unambiguous landmarks (e.g. implanted fiducial markers) within the image can be mathematically erased (i.e. replacing the high contrast voxel values of the landmark with the average voxel intensity of the surrounding voxels) to reduce the bias of the image registration algorithm resulting from the focus of the registration on that high contrast object. A benefit of physical phantoms is that they can be used to test the entire image registration process, including image acquisition with possible distortion and noise, data transfer and import, and image registration. This process is representative of the actual process that is used for patient imaging and image registration.

Virtual phantoms are created or modified from patient images in software. As such, virtual phantoms can be used to test only the image registration process. In many situations it is desirable to have phantom images with precisely known translations and rotations. Introduction of exact rotations and/or translations in virtual phantoms is simple to apply and extremely precise. Also, for digital phantoms, increasing complexity can be generated by adding noise to the image to simulate the realistic variation between image sets.

Both virtual and physical phantoms offer certain advantages and are useful for testing of image registration software and processes. Phantoms can be classified as *rigid* or *deformable* and are used to evaluate the respective registration algorithms. For rigid registration, either physical phantoms (imaged, adjusted by a known amount, and re-imaged) or digital (images that have a known displacement) phantoms can be used. For deformable registration, physical phantoms (with unambiguous points) and digital (images that have a known deformation field applied) can be used. Further classifications can be made based on *imaging modality compatibility* of individual phantoms. It is ideal to have a single phantom that is compatible with all the imaging modalities, which may be used for treatment planning of an individual patient. The final classification is based on *image registration characteristics* that can be evaluated with a specific phantom. Generally, no single phantom is suitable for testing image data integrity, spatial integrity (i.e. accurate dimensions of the voxels and overall image), quality integrity (i.e. accurate display of the voxel values), orientation (i.e. pose of the patient), chirality (i.e. left-right designation in the presence of symmetry), registration accuracy, deformation integrity, and various other system functionalities.

Since CT is the primary imaging modality in RT it is convenient that all phantoms are compatible with CT and the whole phantom including the shell and contents can be imaged without any contrast agents. MR, PET, and SPECT require specialized phantoms that can be filled with contrast agents and often also require fiducial markers. Test objects contained in these phantoms can also be filled with contrast agents (with typically different concentration than the background) or can just be solid objects. In many situations these phantoms can be designed so they are compatible with all three imaging modalities: MR, PET, and SPECT. However, PET and SPECT phantoms present unique challenges due to radioactive contrast agents and multi-modality imaging of these phantoms requires careful planning.

Ultrasound phantoms are highly customized and can be compatible with CT and/or MR. Certain clinical applications require image registration of US and MR images as well. Such phantoms can be created and generally perform very well.

Also, either virtual or physical phantoms used for evaluating image registration accuracy can be classified into two broad categories as *geometrical* (i.e. combinations of standard shapes) or *anthropomorphic* (i.e. representing human anatomy). Well defined dimensions of geometric phantoms make them suitable for testing the spatial integrity of image registration processes, especially when coordinate transformation and voxel interpolation are involved. Geometric shapes are generally easier to accurately position on an imaging device and translate and rotate in precise increments. The main advantage of anthropomorphic phantoms is that they have anatomical features. This is especially important for testing the accuracy of registration algorithms. Use of geometric phantoms for these situations may oversimplify the problem resulting in registration accuracy not obtainable in clinical images. Digital anthropomorphic phantoms can be generated

based on clinical images (e.g. by applying a known deformation to a clinical image) or based on, but independent from, clinical images (e.g. non-uniform rational b-splines (NURBS)-based cardiac-torso (NCAT) phantoms[164]). They are limited by the realism with which they represent human anatomy and many features that are seen in human images are impossible to reproduce in phantoms.

Anthropomorphic deformable phantoms have been developed to validate deformable registration algorithms, including physical phantoms[165-167] and digital phantoms. Physical deformable phantoms are complex, requiring motors to deform the shape and possible computer controllers to introduce deformations in a predictable manner. Deformable phantoms are typically used for intra-modality image registration, mainly kV-CT to kV-CT, CBCT, or MV-CT. Use of deformable phantoms for multi-modality image registration adds complexity, requiring phantoms to have components that are optimized for MR, PET, SPECT, and possibly US. It is considered best practice to ensure that deformation model used to create the digitally deformed image is not the same model that the image set is being used to evaluate.

e. Quality Assurance at Treatment Planning and Re-planning

It is important to note that during commissioning and software upgrade, there are comprehensive quantitative evaluations available because the user has the ground truth in phantom data. There is no comprehensive ground truth when dealing with deformable image registration in patients. Due to this reason, there is no complete voxel-based quantitative evaluation possible to find the true accuracy in patient registration. However, users should evaluate if the transformation is "reasonable" and no obvious error or ill behaviors. Some quantitative evaluations can be performed, such as using the Jacobian determinant method, to screen the transformation matrix for any ill behaviors, however, positive Jacobians do not automatically guarantee the accuracy of the registration. Alternatively, the landmark-based evaluation could be used to evaluate the accuracy of the algorithm if the users can identify corresponding landmarks in two patient images. However, this does not guarantee that the areas without landmarks or between landmarks will be as accurate as the landmark registration indicates. Manual selection of landmarks also carries some uncertainties, especially in low contrast regions.

The validity of the image registration during treatment planning should be assessed following each registration, at a minimum using qualitative assessment tools described in section IV.b. When registration of a second image is used to improve identification of the tumor, the user should evaluate the registration accuracy of the tumor-bearing organ or directly neighboring organs, especially in the case where the tumor itself is not visible on one of the imaging modalities. If the boundaries of the tumor bearing or neighboring organs are not well aligned (as quantitatively or qualitatively determined by the trained reviewer or clinician treating the patient), the uncertainty of the registration (assessed through quantitative or estimated through qualitative techniques) should be included in the PTV margin. For example, in the treatment planning of a liver tumor, if an MR image is being registered to a non-contrast CT (where the tumor is not visible) to enable tumor delineation, the user should assess the correspondence of the liver boundary. Qualitatively, this can be performed by displaying the CT liver contour on the MR and evaluating the accuracy of the

alignment. Quantitatively, the liver could be contoured on the CT and the MR and the mean distance to agreement of the two contours could be calculated. However, it should be noted that alignment of the boundary of an organ between two images does not guarantee that the internal volume of that organ is aligned.

Special care should be used when applying a registration result to a third image. For example, if the CT from a CT-PET scanner is registered to an MR and the transformation is subsequently applied to the PET from the CT-PET, the results should be carefully evaluated. The user should ensure the resulting alignment between the MR and PET is accurate, including first evaluating the alignment of the images obtained from the joined hardware system (e.g. the PET-CT) and the feasibility of the applied registration (e.g. if high activity from the PET is subsequently aligned into bone, this could possibly indicate an area of mis-registration).

The validation for treatment adaptation involves the same components and process described above. Extra care should be taken in the QA process and integration of the registration information into the re-planning process as the anatomical changes between the two images are often substantial and pose a significant challenge to image registration algorithms.

 f. Quality Assurance at Treatment Delivery

The validity of the registration should be assessed prior to treatment, at a minimum using qualitative assessment tools described in section IV.a. In standard clinical practice, registration at treatment delivery is limited to rigid registration to define a translational shift (and possibly a rotation) of the patient to provide a best-fit registration to the planning position. It is often the case that a rigid registration does not align all anatomy due to deformation (i.e. neck flexion in the treatment of a tumor in the head and neck, changes in stomach filling in the abdomen, or changes in bladder/rectum filling in the pelvis). Following the pre-treatment rigid registration, at minimum the alignment of the tumor and critical normal tissues should be qualitatively assessed. If large discrepancies are observed the patient should be re-evaluated, re-positioned, or the physician should be consulted. Semi-quantitative evaluation of the discrepancy between alignment of different tissues is also possible by focusing the registration (through the use of a clip-box, ROI, etc.) on the tumor, then the normal tissues, and comparing the results of the registration. Retrospective assessment of these deviations over a population of patients can help provide information for the generation of planning organ at risk volume (PRV) and PTVs at planning. AAPM Task Group 179 also provides excellent information on the importance of QA at treatment delivery. [168]

V. COMMISSIONING AND VALIDATION OF IMAGE REGISTRATION SOFTWARE

a. Commissioning

As outlined in the previous sections the image registration process is susceptible to errors that can have a serious impact in patient treatment or evaluation. Quality assurance (QA) of the image registration process is essential for the validation of post-transfer image data quality and spatial integrity, image orientation and chirality (i.e. absence of image mirroring), registration and/or deformation accuracy, and other system functionality. As outlined in the AAPM TG53[169] report,

general commissioning and routine procedural quality assurance checks of a multi-modality image registration process used for treatment planning are important to ensure accurate patient treatments.

While it is impractical to address quality assurance of all individual systems and features that are commercially available or developed in house, the tasks described here should be essential elements to any image registration commissioning and quality assurance programs. The exact design of the commissioning process and routine QA tests will depend on individual system features and institutional goals. The overall goal of each QA program should be to ensure that images used for treatment planning, delivery, and evaluation are accurately registered with remaining uncertainties accounted for, free of spatial distortions, and that the overall image quality is preserved through various image manipulations. Furthermore, the QA process should ensure that propagation of patient treatment planning data (contours, interest points, dose distribution) through all image data sets used for plan creation should be consistent and accurate.

Commissioning is performed to investigate the accuracy and reproducibility of the image registration techniques for all sites and imaging modalities prior to clinical use. There are three methods recommended to assess registration results: physical phantom system end-to-end tests, digital phantom tests, and clinical data tests. A comprehensive commissioning process should include all three components. Physical phantom tests enable end-to-end tests to ensure accurate data representation, image transfer, and integrity verification between image acquisition devices, image registration systems, and other radiotherapy systems that use the image registration results. Digital phantoms enable controlled testing of the image registration accuracy (this may also be performed with physical phantoms). Clinical data tests ensure final validation of the accuracy of the system on examples of the images expected in clinical use.

Recommendations from this report are summarized in Table 4.

Table 4. Quality metrics and tolerances for commissioning, annual QA, and patient specific QA for image registration.

Use Case	Quality Metric	Tolerance
Commissioning, Annual, and Upon Upgrade	Data Transfer (including orientation, image size, and data integrity), performed from end-to-end across the entire system using a physics phantom	Exact
	Rigid Registration Accuracy (Digital Phantoms, subset)	Baseline, See details in Table 6
	Deformable Registration Accuracy (Digital Phantoms, subset)	Baseline, see details in Table 6

	Example patient case verification ((including orientation, image size, and data integrity) using real clinical case	Baseline, see details in Table 6
Each Patient	Data transfer	Exact
	Patient orientation	Image Data matches specified orientation (Superior/Inferior, Anterior/Posterior, Left/Right)
	Image size	Qualitative – no observable distortions, correct aspect ratio
	Data Integrity and Import	User defined per TG53 recommendations
	Contour propagation	Visual confirmation that visible boundaries are within 1-2 voxels of contours
	Rigid registration accuracy	At Planning: confirmation that visible, relevant boundaries of anatomy in the registered images are within 1-2 voxels of the registered image; additional error should feed into margins At Treatment: confirmation that visible boundaries are within PTV/PRV margins (doesn't account for intrafraction motion)
	Deformable registration accuracy	At Planning: confirmation that visible, relevant boundaries and features of anatomy in the registered images are within 1-2 voxels of the registered image; additional error should feed into margins; evaluate reasonableness of the deformation vector field; perform quantitative evaluation if results are questionable or if accuracy requirements are significant (e.g. SBRT, dose mapping for critical tissues) At Treatment: confirmation that visible boundaries are within PTV/PRV margins (doesn't account for intrafraction motion)

i. Software system specific validation

Validation of image registration software performance can be divided into two broad areas, i) validation of image transfer and data integrity between different systems and ii) validation of the actual image registration functionality and accuracy. The data transfer integrity is also performed

and recommended as a part of general commissioning of treatment planning systems and imaging devices used in RT. [165,166] Changes in configuration of software or hardware or upgrades of any scanner, computer, or network associated with the RT planning have a potential of introducing errors and disturbing established communications. Prior to upgrading or modifying any of the components, there should be a communication regarding which processes may be disturbed and appropriate arrangements should be made for end to end testing following the changes. Chapter 7 of the AAPM TG53 report discusses in detail issues related to management of treatment planning systems and networks. The RT QA program should identify individuals responsible for system management and should include tests for validation of proper communication after system modifications. That component of the comprehensive RT QA program should already be in place based on AAPM TG53 and TG66 recommendations and should satisfy the needs of a multimodality image registration program.

Previously, in Section IV.e, phantoms were described for use in validation of image registration software. These phantoms can be classified as virtual or physical phantoms. Virtual phantoms can be used for performance of all tests outlined in Table 4. These tests range from validation of very basic rigid registration to more complex deformable registration and are the main focus of this report. Physical phantoms are needed for end-to-end tests and for validation of data transfer integrity as they can be physically imaged on various imaging devices and then images of these phantoms can be transferred through the image registration process, simulating the actual steps that are used for patient data processing.

ii. System end-to-end tests with physical phantom

It is the recommendation of this task group that an end-to-end test be performed during the commissioning, annually, at an image acquisition device repair or replacement with the potential to impact data integrity, or at each major image registration software upgrade, which is consistent with TG53[169] and IAEA-430[170]. The performance of end-to-end tests is a critical component to ensure the accuracy and consistency of the overall function of the image acquisition, registration, and planning/delivery procedure. If the registration is a stand-alone system, integrated between other components, e.g. the imaging devices and the treatment planning system, the end-to-end tests ensure compatibility and accuracy. It is also the recommendation of this task group that a simple end-to-end test is performed annually. For smaller, single physicist clinics, this provides the opportunity to invoke a 'time out' for validation. For larger clinics, it ensures that the overall process has not been altered without the knowledge of the physicist responsible for the registration component.

A multi-modality (if necessary) physical phantom with unambiguous internal landmarks and orientation should be imaged on each scanner in head first supine, head first prone, feet first supine, feet first prone orientations, and combination of decubitus and head/feet first orientations. It is important that each patient orientation be selected when programming individual image acquisition sequences so the individual orientations of the phantom are listed in DICOM headers of acquired images and then the correct identification and manipulation of each patient (image) orientation by the image registration software can be verified. The images should be imported into the image registration software and the correct orientation and image labeling should be verified. Image

registration between individual devices should be performed using standard clinical protocols. Accuracy of the registration should be assessed by evaluating the registration of unambiguous landmarks in the phantom.

The reliability of image and other data communications between different hospital systems has been greatly simplified with wide acceptance of DICOM standard by various manufacturers. While these systems have come a long way, incompatibility and implementation differences of DICOM standards among various manufacturers are still frequent sources of errors, and image transfer tests should be performed to verify proper transfer and processing of DICOM objects. These tests should verify that images transferred from a scanner (CT, MRI, PET, SPECT), Picture Archiving and Communication System (PACS), or treatment machine preserves the following items in the receiving image registration system: pixel size, slice thickness and spacing, orientation (i.e. head/feet first, supine/prone, left/right), scan text information, and voxel value.

Correct transfer and interpretation of image parameters should be verified during the commissioning process and after all software and hardware upgrades as well as for each individual patient. Often, secondary treatment planning datasets are acquired at various outside institutions and evaluation of data transfer from these systems cannot always be performed during commissioning. Validation of such dataset transfer should then be performed on an individual patient basis.

A) Validation of correct image geometry - Transfer of data between systems that display images in different resolution or apply transformations to pixel locations can affect image geometry due to pixel averaging, down-sampling, and various other reasons.

Validation of correct image geometry requires a phantom with test objects spaced at known distances throughout the phantom. The test involves scanning of the phantom with typical clinical protocols, image transfer, and measurement of separations between the test objects. Validation should be performed on each individual software package where contouring or treatment planning work is performed with the evaluated images. The test objects should be placed so that the correct image geometry can be evaluated in all three dimensions. The measurements should be accurate to ½ the size of the voxel in the measurement direction. It is important to note that spatial distortions are not necessarily uniform and may demonstrate only in one dimension. Validation of image size in three dimensions ensures correct pixel size, slice thickness and spacing, and overall spatial fidelity. As already described, MRI images may contain inherent spatial distortions, which should be separated from these tests. Other imaging modalities should not contain detectable distortions.

The aim of the image geometry tests is to evaluate image geometrical distortions due to data transfer between systems and not the inherent image distortions. If significant distortions are observed in the transferred data, it should be first validated that these distortions are not present when viewing images on the scanner console before proceeding with further testing. If the distortions are inherent to the scanner, data transfer validation should be repeated after the problem is rectified.

B.) Validation of Correct Image orientation- Validation of correct image transfer orientation should be performed for all clinically used patient positioning orientations. A non-symmetrical phantom or a phantom with fiducial markers should be scanned with all the clinically used patient orientation combinations. Typical combinations are head first/supine; head first/prone; feet first/supine, feet first/prone, and combination of decubitus and head/feet first orientation. A successful test results in the correct right/left, head/feet (superior/inferior), and anterior/posterior labeling assigned to the transferred patient images, and all graphical orientation indicators are correct.

Commissioning is also the best time to establish routine use of image orientation fiducials placed either permanently on a scanner, a treatment machine couch, or directly on patients. The use of such fiducials is strongly recommended for all imaging procedures used in the RT patient treatment process. Systematic use of orientation markers can reduce likelihood of potentially serious treatment errors. The use of such markers is relatively straightforward in CT; TG66 has recommended that two thin aluminum wires be taped on the bottom of the CT scanner tabletop to indicate patient orientation in CT images. The wires should be taped on the left or right side of the tabletop and along its entire length. The two wires should also form the letter "V" which is pointing towards the gantry. The letter "V" indicates patient's scan orientation (Head/Feet first). The wires should be small enough to avoid image artifacts. Such wires can be used on treatment machine couches as well. Use of couch mounted markers for MR, PET, and SPECT imaging is much more difficult due to nature of image acquisition and patient specific fiducials are an optimal solution for these modalities.

C) Validation of Correct Image Parameters and Spatial Accuracy

Image files contain patient demographic information, image acquisition parameters, image orientation, voxel size, voxel locations, and individual voxel values. While DICOM standards greatly improve accuracy of transferred image data sets, it is possible that one or several of the above parameters can become corrupt or misinterpreted during transfer.

iii. Digital Phantom Tests

Digital phantoms can be developed in house or purchased from vendors. The following digital phantom data, shown in Table 5, have been generated by this task group for use in commissioning and quality assurance programs for image registration accuracy tests. The datasets were generated using ImSimQA™ software (Oncology System Limited, UK (OSL)). The datasets, or equivalent datasets, should be imported into the image registration software and the tests outlined in Table 4 should be performed. An alternating subset of these datasets should be used for testing annually or at time of upgrades. Image registration using the datasets in Table 5 should be performed in the clinical image registration system, as necessary per clinical activity.

Table 5. Digital Phantom Data Set Generated by ImSimQA™ software (Oncology System Limited, UK (OSL)). (HFS: head first, supine; HFP: head first, prone; FFS: feet first supine; FFP: feet first prone)

DATASET	DESCRIPTION
Basic Phantom Dataset - 1	Reference dataset - HFS - Black image with white and 3 shades of grey images. The voxel dimensions of all basic phantom datasets are 0.7 x 0.7 x 3 mm. Cone pointing superior, semi-circle on right side, cube anterior to cylinder, 3 skin markers, and 3 internal markers, all in the same reference frame with defined perfect registration by generation of images with the following parameters: CT PET MRI-T1 weighted (TR=500ms, TE=12ms) MRI-T2 weighted (TR =4000ms, TE = 120ms) CBCT (with noise added)
Basic Phantom Dataset - 2	Same as Basic Phantom Dataset - 1 -CT - with the following offsets: To left = 1.0 cm, To anterior = 0.5 cm, to Inferior = 1.5 cm
Basic Phantom Dataset - 3	Same as Basic Phantom Dataset - 1 - CT - with the following offsets: To left = 0.5 cm, To anterior = 1.5 cm, to Inferior = 2.0 cm, rotation = -5° about X-axis, +8° about Y-axis, +10° along Z-axis
Basic Phantom Dataset - 4	Same as Basic Phantom Dataset - 1 - CT - except it is FFS
Basic Phantom Dataset - 5	Same as Basic Phantom Dataset - 1 - CT - except it is HFP
Basic Phantom Dataset - 6	Same as Basic Phantom Dataset - 1 -CT - except it is FFP
Basic Anatomical Dataset -1	Reference Dataset – CT – HFS - the Pelvis phantom provided by ImSimQA™ software (Oncology System Limited, UK (OSL)) with 3 markers in the region of bladder, prostate, and rectum. The voxel dimensions of the CT, CBCT, and PET basic anatomical datasets are 0.91 x 0.91 x 3 mm. The voxel dimensions of the MR basic anatomical datasets are 1.83 x

	1.83 x 3 mm.
Basic Anatomical Dataset -2	Same as Basic Anatomical Dataset -1 – CT - with offsets of: To left = 0.3 cm, To anterior = 0.5 cm, To inferior = 1.2 cm
Basic Anatomical Dataset -3	Same as Basic Anatomical Dataset -1 - PET – HFS - with offsets of: To left = 0.3 cm, To anterior = 0.5 cm, To inferior = 1.2 cm
Basic Anatomical Dataset -4	Same as Basic Anatomical Dataset -1 - MR-T1 – HFS - with offsets of: To left = 0.3 cm, To anterior = 0.5 cm, To inferior = 1.2 cm
Basic Anatomical Dataset -5	Same as Basic Anatomical Dataset -1 - MR-T2 – HFS - with offsets of: To left = 0.3 cm, to anterior = 0.5 cm, to Inferior = 1.2 cm
Basic Deformation Dataset - 1	Same as Basic Anatomical Dataset - 1 with added Gaussian noise variation and the following global offsets: To left = 0.3 cm, to anterior = 0.5 cm, To inferior = 1.2 cm. Three markers were set inside the prostate regions, prostate volume increased by105%, -10° rotation about X-axis, +10° rotation about Y-axis, +10° rotation about Z-axis.
Sliding Deformation Dataset - 1	Reference dataset – HFS – True anatomical CT set of lung (courtesy of the DIR Lab, www.dir-lab.com/4DCT6.html)
Sliding Deformation Dataset - 2	Same as Sliding Deformation Dataset - 1, deformed image is generated with added noise variation, no overall offset (i.e. 4D CT), diaphragm motion of 1.5 cm SI, and tumor motion 1.0 cm SI, 0.5 cm AP. Tumor is solid, small, and mid-lung.
Clinical Lung Dataset – End Exhalation and End Inhalation	DIR Lab 4D CT dataset (end exhalation and end inhalation reconstruction only) with semi-automatically selected bifurcation points

The following Table 6 describes the tests and suggested tolerances for the rigid and deformable registration accuracy tests, for the digital phantom data described in Table 5. Deformable registration algorithms are currently an area of active research and commercialization. The selection of these tolerances was driven by the clinical experience of the task group and published validation

studies.[171-173] For example, a multi-institutional study on clinical 4D CT lung data showed that 18 of the 21 participants could achieve a mean absolute error of 2.0 mm or less and 9 algorithms had a maximum error of less than 5.0 mm in each direction.[174] The tolerances listed are goals. If an algorithm does not meet the stated tolerance at commissioning, limitations should be noted and expected uncertainties should be included in treatment protocols. Areas of larger expected uncertainties and algorithm limitations should be communicated to the multi-disciplinary team.

Table 6: Recommended tests and tolerances for the digital phantom test cases. See Table 4 for recommended testing schedule. Here the voxel dimension should be the calculated as the 3D vector magnitude of the image with the largest voxel size to reflect the non-isotropic size of most imaging voxels.

Stationary Image	Moving Image	Test	Tolerance
All Datasets		Voxel Intensity Orientation	Exact Exact
Basic Phantom Dataset - 2	Each modality image in Basic Phantom Dataset – 1	Rigid Registration – Translation Only	Maximum cardinal direction error less than 0.5*voxel dimension
Basic Phantom Dataset – 3	Each modality image in Basic Phantom Dataset – 1	Rigid Registration – Translation and Rotation	Maximum cardinal direction error less than 0.5*voxel dimension
Basic Anatomical Dataset - 1	Basic Anatomical Dataset - 2	Registration – translation only	Maximum cardinal direction error less than 0.5*voxel dimension size
Basic Anatomical Dataset - 1	Basic Anatomical Dataset - 3	Registration – translation only	Maximum cardinal direction error less than 0.5*voxel dimension size
Basic Anatomical Dataset - 1	Basic Anatomical Dataset - 4	Registration – translation only	Maximum cardinal direction error less than 0.5*voxel dimension size
Basic Anatomical Dataset - 1	Basic Anatomical Dataset - 5	Registration – translation only	Maximum cardinal direction error less than 0.5*voxel dimension size
Basic Anatomical	Basic Deformation	Deformable	95% of voxels within the

Dataset - 1	Dataset - 1	Registration	phantom within 2 mm max error less than 5 mm
Sliding Deformation Dataset - 1	Sliding Deformation Dataset - 2	Deformable Registration	95% of voxels within the phantom within 2 mm Max error less than 5 mm
Clinical 4DCT dataset	(Deformation can be processed in either direction)	Deformable Registration	Mean vector error of all landmark points less than 2 mm Max error less than 5 mm

Evaluating the accuracy of the deformation phantom should be performed using the DICOM deformation vector field (DVF) files. As stated in Section IV.a, image registration algorithms should export a DICOM DVF. The applied deformation is available on the AAPM website for the test phantoms. The user should then subtract the DICOM images for each direction (i.e. the LR, AP, and SI directions are individual DICOM files) and determine the percentage of voxels that are within the tolerance

iv. Example Clinical Data Tests

Once the standard operating level of the registration software is assessed using the end-to-end tests on the physical phantoms and the comprehensive validation using the digital phantoms, an evaluation of the registration accuracy should be performed using example clinical datasets. These tests should be designed based on the clinical protocols at each institution using the quantitative and qualitative metrics described in Sections IV.b and IV.c.

For example, if a clinical protocol is planned to use deformable image registration to propagate contours defined on one phase of a 4D CT onto all other phases of the 4D CT for lung tumor planning, an example set of 4D CT images should be collected from the clinic (e.g. 10 4D CT image sets obtained from typical patients previously treated in the clinic). The planned registration protocol should be performed on these 10 datasets and the results should be evaluated using the quantitative and qualitative verification techniques described in Sections IV b and c. The magnitude of the registration uncertainties resulting from these tests should be incorporated into the treatment protocols (e.g. into the uncertainty margins).

b. Patient specific registration verification during clinical practice

Even the most comprehensive commissioning of the image registration algorithm cannot capture the entire scope of registration challenges that will be encountered in the clinic. A well-documented patient specific verification protocol for routine practice is therefore essential as the image registration is used for many activities during the radiotherapy planning and treatment. Frequently, the registration is performed by one team member for use by another member for various tasks,

therefore documentation of the registration technique and patient-specific accuracy is essential to ensure appropriate treatment of the patient.

Communication regarding the needs and results of the image registration between the multi-disciplinary team is essential for the safe and efficient integration of image registration in radiotherapy. The most effective procedure for ensuring effective communication depends on clinic size and structure. This task group recommends an image registration directive analogous to treatment planning directives. The two main communication interactions to address are **the request and the report**. The request for an image registration procedure should clearly identify the intended use of the result as well as indicate the region(s) of greatest importance. Also, when the registration is performed at a time prior to the use of the registration, the registration results should be reported back to the multi-disciplinary team with appropriate indications of the accuracy of the registration and in which local regions unusable results. Each use case poses its own challenges and requirements, but in every case, clinical errors can be made if the communications related to image registration are misinterpreted. Language is proposed in Table 7 to describe the accuracy of an image registration.

In general, the following elements of communication should be exchanged:
1) Request
   a. Clear identification of the image set(s) to be registered
      i. Explicit identification of the primary reference image and the images to register to it
   b. An understanding of the local region(s) of importance
      i. Anatomical regions and target location(s) or
      ii. Local landmarks or
      iii. Bounding box or other indicators on image
   c. The intended use of the result
      Examples:
      i. Target delineation
      ii. Dose compositing (re-treatment)
      iii. 4D change assessment (normal and tumor tissue)
   d. Techniques to use (appropriate for the intended use
      i. Deformable
      ii. Rigid

   e. The accuracy required for the final use:
      i. Explicitly stated or
      ii. Implicitly defined by therapy plan scenario (e.g. stereotactic) or
      iii. Implicitly defined by intended use

2) Report
   a. Identify actual images used
   b. Indicate the uncertainties in the final registration for local regions of importance and anatomical landmarks
      i. Identify any critical inaccuracies to alert the user
   c. Verify acceptable tolerances for use
   d. Techniques used to perform registration
   e. Sample fused images in report with annotations
   f. Documentation from system used for fusion

Appendix B provides examples of an **Image Registration Request and Report form.**

Table 7. Registration uncertainty assessment level and description.

Uncertainty Assessment	Phrase	Description
0	Whole scan aligned	- Anatomy within 1 mm everywhere - Useful for structure definition everywhere - Appropriate for stereotactic localization
1	Locally aligned	- Anatomy local to the area of interest is un-distorted and aligned within 1mm - Useful for structure definition within the local region - Appropriate for localization provided target is in locally aligned region
2	Useable with risk of deformation	- Aligned locally, with mild anatomical variation - Acceptable registration required deformation which risks altering anatomy - Registered image shouldn't be used solely for target definition as target may be deformed - Increased reliance on additional information is highly recommended - Registered image information should be used in complimentary manner and no image should be used by itself
3	Useable for diagnosis only	- Registration not good enough to rely on geometric integrity - Possible use to identify general location of lesion (e.g. PET hot spot)
4	Alignment not acceptable	- Unable to align anatomy to acceptable levels - Patient position variation too great between scans (e.g. surgical resection of the anatomy of interest or dramatic weight change between scans)

VI.   CLINICAL INTEGRATION OF REGISTRATION TECHNIQUES IN TREATMENT PLANNING AND DELIVERY

The clinical integration of successful image registration programs should provide an efficient and safe practice. In order to ensure the safe use of image registration, this task group recommends the following steps:

1) Clear guidelines are provided to the personnel implementing the image registration,
2) An efficient, patient specific verification is performed for each image registration prior to its use (e.g. qualitative assessment of registration results),
3) Registration accuracy is assessed at a frequency to minimize the effect of errors without prohibiting clinical flow,
4) Clear identification of the accuracy of the registration is provided to the consumer of the image fusion so they are fully aware of and can account for any uncertainties.

Commercially available systems provide advanced tools for image registration and fusion. In order to improve usability by a variety of users, the complexity, and often the algorithms, is hidden from the user. The resulting risk is that the commercial systems provide capabilities to users that may not be fully understood. The inappropriate use of these technologies can lead to potential errors in the treatment process. It is likely that all members of the multi-disciplinary radiotherapy team will use or request the results of the registration system. However, comprehensive knowledge of the algorithm and its limitations cannot be assumed for all personnel. Therefore, for clinical implementation, it is the responsibility of the physicists to ensure proper training of the personnel performing the image registration, that the personnel have an adequate understanding of how to use the system for each particular patient case, and that the algorithm is used in a safe manner, accounting for its uncertainties and limitations.

In addition, a patient specific registration verification process should take place before the resulting data is used in the clinic. This might include quantitative measurements as described above in Section IV.c, but should always include a qualitative evaluation across the entire dataset, described in Section IV.b. This patient specific quality check serves to provide confidence to the user and helps to ensure safe operation of these systems. In clinical practice, this verification should be communicated to consumers of the results of the registration.

a. Treatment Planning

The first critical component of image registration for treatment planning is a consistent patient position between all imaging studies. For this reason, it is highly desirable to have a process that allows imaging of the patient in the treatment position, and ideally in the immobilization used for treatment. This is not always practical, but any steps that can be made to better align the patient positions between multi-modality imaging and that used for treatment is beneficial to the program. External fiducial marker placement may also assist in the preparation.

Second, it is the recommendation of this task group that a trained member of the radiotherapy team perform the image registration and fusion prior to treatment planning. This person may also generate the report and recommend a level of uncertainty assessment, defined in Table 7.

Third, the user of the registration results (i.e. the radiation oncologist) should assess the registration accuracy and any tradeoffs made in the registration using methods described in Section IV b and c. The final review of the image registration for clinical use by the treating radiation oncologist is analogous to the final review of the dosimetric planning tradeoffs made by the radiation oncologist

Fourth, residual error in the registration that cannot be resolved should be accounted for, e.g. in the treatment margins (PTV).

As an example, referring back to the MR-CT registration for liver cancer described in IV.ii.1. If an MR image is registered to a CT for treatment planning, and the MR is used to delineate the GTV and the CT is used to delineate the normal tissues and calculate the dose, an assessment of the registration accuracy should be performed. This could be a visual evaluation of the liver boundary using a checkerboard technique or comparison of the spatial location of an identifiable marker (i.e. a clip or a branch in a blood vessel) on both images. If notable discrepancies are detected (i.e. greater than the voxel size) the uncertainty should be estimated (by measuring the distance between the boundaries of the liver or the difference in location of the marker). The closer the measured uncertainty is to the GTV the more representative it will be of the GTV registration accuracy. It may be appropriate to account for this uncertainty as a potential systematic error in the process. There are different philosophies that describe the incorporation of these uncertainties into the treatment margin, e.g. linear addition of the uncertainties or addition in quadrature, and a clear consensus within the radiation oncology community has not been reached.

b. Treatment Delivery

For each treatment site, a written protocol (e.g. registration request) should be developed providing a description of what aspects of the image should be aligned for treatment and identification of landmarks that can be used for verification. For example, for prostate, one may want to align the prostate rectum boundary for treatment, and use the apex of the prostate for verification. Image registration for treatment delivery is typically performed and applied by the same team of users; therefore the communication of the registration results can be performed verbally within the team. It is imperative that the users are trained on how to quickly verify the accuracy. A detailed protocol will provide a guide for therapists, and will make the registration process consistent for every patient case. If image guidance is to be used for an uncommon case for which no protocol has been developed, a clear directive of what is to be aligned for treatment and what accuracy is required should be provided to the therapists prior to the onset of treatment or the physician should evaluate the registration prior to treatment.

This task group recommends that the radiation therapist, adequately trained in image registration and the specific protocol, perform the image registration for treatment delivery. This will facilitate efficient integration of image registration into the treatment delivery process. Final validation and use of image guidance should be decided on an institutional and protocol specific basis based on the training and experience of the multi-disciplinary team, the interplay between the IGRT technique and treatment margins, and regulatory guidelines. It is important that clinical operating principles be developed to avoid complacency and ensure efficient and safe treatment for patients. For final validation of image guidance for standard dose fractionation, it is often recommended that the

radiation oncologist approve each image registration used for treatment prior to the subsequent treatment fraction delivered to the patient. Special consideration should be given to higher fractional doses, greater than 5Gy, such as that used in stereo-tactic radiosurgery. The current recommendation from the American Society for Radiation Oncology (ASTRO) and American College of Radiology (ACR) Practice Guideline for the Performance of Stereotactic Body Radiation Therapy is for approval of the image registration prior to delivery of the radiation by a radiation oncologist.[175]

c. Treatment Monitoring and Adaptation

Recently, the development of deformable image registration platforms has enabled sophisticated treatment monitoring, including dose accumulation in deforming anatomy, e.g. the quantification of the dose delivered to sub-units of the tissue over the course of treatment accounting for variations in position and shape of organs through deformable registration, and the ability to perform more sophisticated adaptive re-planning when anatomical or functional changes in the patient are observed.

The validation requirements for this clinical process include those described above for both treatment planning and image guidance. Verification of each image registration should be performed prior to the use of the registration to accumulate the dose. However, it is important to note the use of deformable registration to accumulate dose has additional demands on accuracy compared to the use of deformable registration for contour propagation. For dose accumulation, the correspondence of every voxel receiving significant dose should be accurately aligned, whereas for contour propagation the accuracy is most important at the boundary of the organ. The use of deformable registration for dose accumulation and subsequent adaptive re-planning is outside of the scope of this task group. It is recommended that these issues be addressed in a subsequent task group. Protocols should be defined to guide the process for each treatment site, accounting for expected uncertainties and ensure detection of unexpected levels of uncertainties. In addition, when using image registration for treatment adaptation or retreatment of patients where there is a risk of exceeding normal tissue toxicity levels, the multi-disciplinary team should discuss the uncertainties and limitations of the image registration. This is currently an area of rapid innovation and caution should be used when employing these new techniques until they are well understood.

d. Clinical Case Illustrations

i. Target and Critical Structure Segmentation at Planning

Below are two clinical case illustrations for the planning request for image registration for structure segmentation, the results of the registration, and the subsequent report.

1. A spinal stereotactic procedure is to be performed for two lesions in T2 and T7 vertebral bodies. The physician has reviewed the diagnostic MRI scans with 1 mm voxel resolution and requests that they be registered to the treatment planning CT scan, with 1 mm slice thickness, to identify the target volumes for treatment. In this case the request should include the following information

Request
- Which MRI scan(s) from which study (i.e. Sagittal T1 axial post gad)
- Treatment Planning CT is the primary
- Regions of T2 and T7 vertebral bodies are most critical
- Intended use is target definition for stereotactic RT
- Rigid registration should be used to avoid deforming the tumor
- Desired accuracy is on the order of 1 mm to be consistent with the expected 1 mm accuracy of alignment at treatment

Upon performing the image registration, it was noticed that the spine was arched more in the MRI making it impossible to align both T2 and T7 vertebral bodies with a single rigid registration. It was decided to use two separate rigid registrations to accomplish the goal.

Report
- Sagittal T1 axial post gad was registered with the treatment planning CT
- Two separate rigid registrations were performed, one to align T2 and the other to align T7
- Accuracy is on the order of 1 mm was obtained for the vertebral bodies, determined by evaluating boundary of the boney structure and small, point like calcifications

The registration was approved; the target was contoured on the fused dataset using the fusion that was appropriate for each vertebral body. No expansion was applied for the registration uncertainty.

2. A liver patient is contrast intolerant and has a prior MRI scan that clearly identifies the lesions in the left lobe to be treated. The MRI was acquired in an arbitrary voluntary breath hold state and the patient is to be treated at an externally assisted exhale breath-hold state.

Request
- Which MRI scan(s) from which study (i.e. Sagittal T1 axial post gad)
- Treatment Planning CT is the primary
- Left lobe of the liver is the most critical
- Intended use is target definition
- Uncertainty in registration should be reported and added to the PTV margin

Upon performing the registration, it was noted that deformation was present between the MR and CT scans. The registration focused on the left lobe containing the tumor. The left lobe of the liver aligned very well, the boundary of this lobe matched to within the voxel size.

Report
- T2 axial MR was registered with the treatment planning CT
- Rigid registration focused on the left lobe, for purposes of tumor definition
- Accuracy on the order of 2 mm was obtained for the left lobe

The registration was approved, the tumor contour was generated based on the fused MR, and no expansion was deemed necessary for the registration uncertainty.

ii. Target Registration and Normal Tissue Avoidance at Treatment Delivery

The use of image registration in the treatment room should be designed within the whole context of the planning and delivery workflow. An example workflow is shown in Figure 6. Currently, standard in room image guidance requires a single translation (plus possible rotation) to be applied to the patient. This constraint in using the image registration requires tradeoffs in the registration process (i.e. the distribution of the residual errors following registration). These tradeoffs should be accounted for in the planning process (e.g. if targeting the tumor is the primary focus at treatment, a PRV may be necessary at planning to ensure that the normal tissue is not overdosed). Advances in the field may reduce these requirements through the use of adaptive and real-time, in room planning. The template for guidance shown above illustrates the need for image registration and assessment of registration in the treatment room.

Following patient setup and acquisition of the in-room image, the field of view should be set for the image registration. This may be the entire image, a specific region of interest (e.g. the tumor), or a larger region of interest (e.g. the entire neck). Once the field of view is set, the registration technique should be selected, this should be designated in a treatment protocol for the patient or class of patients. This should include the similarity metric, transformation algorithm, and optimization technique (as applicable). Following registration, the shift should be assessed to decide if the magnitude is within specification and treatment should move forward or if an intervention should occur (e.g. reset up the patient). If moving forward, the registration accuracy should be assessed. It is important at this step that the registration accuracy is assessed everywhere, not just within the specific region of interest, to ensure that normal tissue avoidance is maintained. The plan adequacy should be evaluated (e.g. with the applied correction, can the intended plan be delivered to within an allowable level of deviation). These criteria will vary based on treatment site, protocol, and institution.

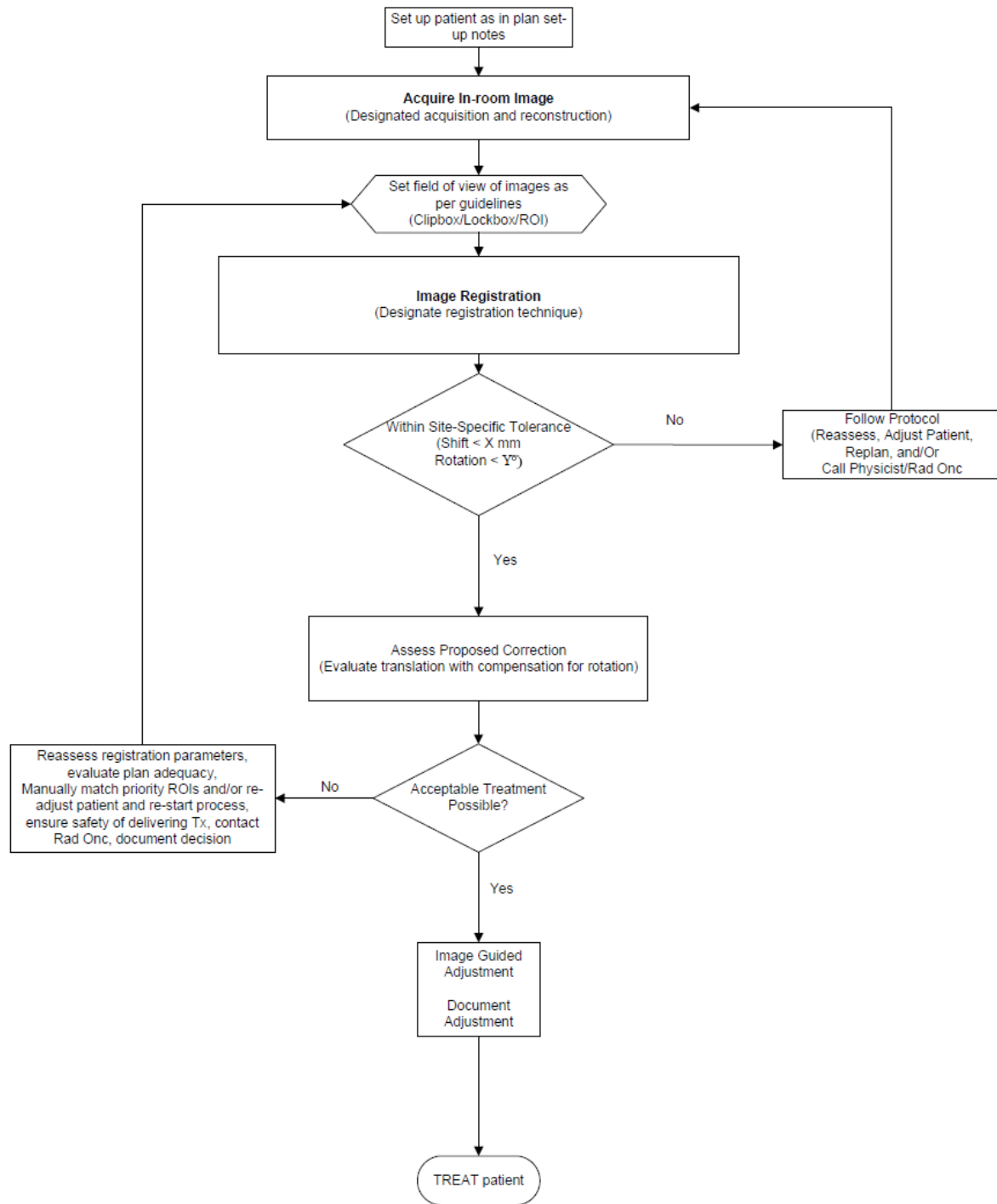## Image Registration and Guidance Protocol at the Treatment Unit

Figure 6. Summary of an example image guidance protocol

VI. CONCLUSIONS

Image registration and fusion has the potential to improve the planning, delivery, and assessment of radiotherapy. However, as with any advanced technology used in the treatment of patients, it should be commissioned and integrated into the clinic in a safe and efficient manner. As the complexity of the registration increases the validation, quality assurance, and verification methods needed in the commissioning and clinical integration of the software also increases. As described in this task group report, the commissioning and quality assurance program associated with an image registration application is multifaceted. Only through the combination of multiple tests, can a complete assessment of the accuracy be obtained.

At the time of publication of this document, the tools needed to complete all recommended commissioning steps outlined in this report are not standard in all commercial algorithms. The purpose of this report is to also provide guidance to the vendors on the tools that are needed to efficiently perform these tasks within the commercial system.

The recommendations of this task group can be summarized as follows:
Clinical Recommendations:
1. Understand the basic image registration techniques and methods of visualizing image fusion
2.   Understand the basic components of the registration algorithm used clinically to ensure its proper use
3. Perform end-to-end tests, using a physical phantom, of imaging, registration, and planning/treatment systems if image registration is performed on a stand-alone system
4. Perform comprehensive commissioning of image registration using the provided digital phantom data (or similar data) as well as clinical data from the user's institution
    a. Estimation of registration error should be assessed using a combination of the quantitative and qualitative evaluation tools described in Tables 3 and 4. Regions with larger estimated errors should be accounted for in the uncertainty margins used.
5. Develop a request and report system to ensure communication and documentation between all users of image registration
6. Establish a patient specific QA practice for efficient evaluation of image registration results

Vendor Recommendations:
1. Disclose basic components of their registration algorithm to ensure its proper use
2. Provide the ability to export the registration matrix or deformation vector field for validation
3. Provide tools to qualitatively evaluate the image registration
4. Provide the ability to identify landmarks on 2 images and calculate the TRE from the registration
5. Provide the ability to calculate the DSC and MDA between the contours defined on an image and the contours mapped to the image via image registration
6. Support the integration of a request and report system for image registration

This task group report aims to provide a comprehensive, yet feasible, commissioning and QA system. The image registration system should be commissioned for clinical use, as per all other devices in the clinic. It is essential that the physicist understand the fundamental components of the algorithm to ensure its safe and appropriate use in the clinic. In addition to commissioning, a quality assurance

process should be in place to ensure that the clinical use of the registration is appropriate. The tests described in this report propose guidelines for both the frequency and tolerance recommended to aid in the safe and effective use of image registration in the clinic. The individual protocols for each clinical department will drive further tailoring of these guidelines to include the additional steps necessary for safe execution of the use of image registration.

VI.   APPENDICES

APPENDIX A. Recommended anatomy to qualitatively assess image registration on a site-specific basis.

Image Registration

Site	Anatomical Landmark Match
Brain	Orbits, Optic Nerves, Brainstem, Ventricles, Sella Turcica, Nose, External Auditory Canal (may be useful for minimizing rotation/roll), and Clivus (for minimizing rotation/yaw errors) Sagittal Suture
Head and Neck	If anterior facial tumor, fuse by Maxilla, Brainstem and Orbits and Nose
Neck	Cervical Spine (one vertebral body above and below treatment site)
Chest	T-Spine or L-Spine near the area
Chest Wall	Adjust T-Spine in the area of treatment , then adjust to the closest ribs or by sternum
Abdomen	Liver, spleen, and/or kidney boundary Axial alignment of the abdominal aorta
Hand	Metacarpals or phalanges
Wrist	Carpal Bones
Long Bones	Fuse joint to joint. If only one joint available, start there. Femoral head or humeral head depending on tumor location.
Pelvis	Symphysis Pubis, Sacroiliac Joint, Sacrum,

	Iliac Crest, Femoral Head (may be useful for minimizing rotation/roll) Prostate cancer: Prostate, penile bulb
Foot	Calcaneus and Tarsals or Metatarsals only if foot is flexed

APPENDIX B. Example templates of an image registration request and report.

Image Registration Request

Primary Reference Image

o Simulation CT   o MRI   o PET   Date_____   Details_____

Images to be registered to the primary reference image

o CT   o PET   o MRI (o sag o cor o axial) Date_____   Details_____

o CT   o PET   o MRI (o sag o cor o axial) Date_____   Details_____

Intended Use

o Target or structure delineation   o Dose compositing

o Motion management   o Disease progression or response

Comment: _____

Local Regions of Importance

	Region	Comment	Landmarks
1.	_____	_____	_____
2.	_____	_____	_____
3.	_____	_____	_____
4.	_____	_____	_____

Registration Technique

o Rigid Only   o Rigid and Deformable   o Deformable only

Accuracy Requirements

◯ 0: Whole Scan Aligned

◯ 1: Locally Aligned

◯ 2: Useable if deformation exists (registered image for complimentary information only)

◯ 3: Registration for diagnosis only (registration needed to identify general area)

Comment: _____

Requesting Physician: _____

Date: _____

Signature: _____

Image Registration Report

Primary Reference Image:

Modality_____ Date_____ Details_____

Images to be registered to the primary reference image

Modality_____ Date_____ Details_____ Technique_____

Modality_____ Date_____ Details_____ Technique_____

Intended Use

o Target or structure delineation   o Dose compositing

o Motion management   o Disease progression or response

Comment: _____

Local Region Alignment Accuracy

	Region/Metric	Accuracy Level	Comment	Screen Shot
1.	_____	_____	_____	o
2.	_____	_____	_____	o
3.	_____	_____	_____	o
4.	_____	_____	_____	o

Accuracy Level

◯ 0: Whole Scan Aligned

○ 1: Locally Aligned

○ 2: Useable with risk of deformation (additional PTV/PRV margin may be required)

○ 3: Useable for diagnosis only (registration only suitable to identify general area)

○ 4: Alignment not acceptable (Do Not Use!)

Comment: _____

Notes:_____
_____
_____

Clinician Performing Registration: _____

           Signature: _____ **Date:** _____
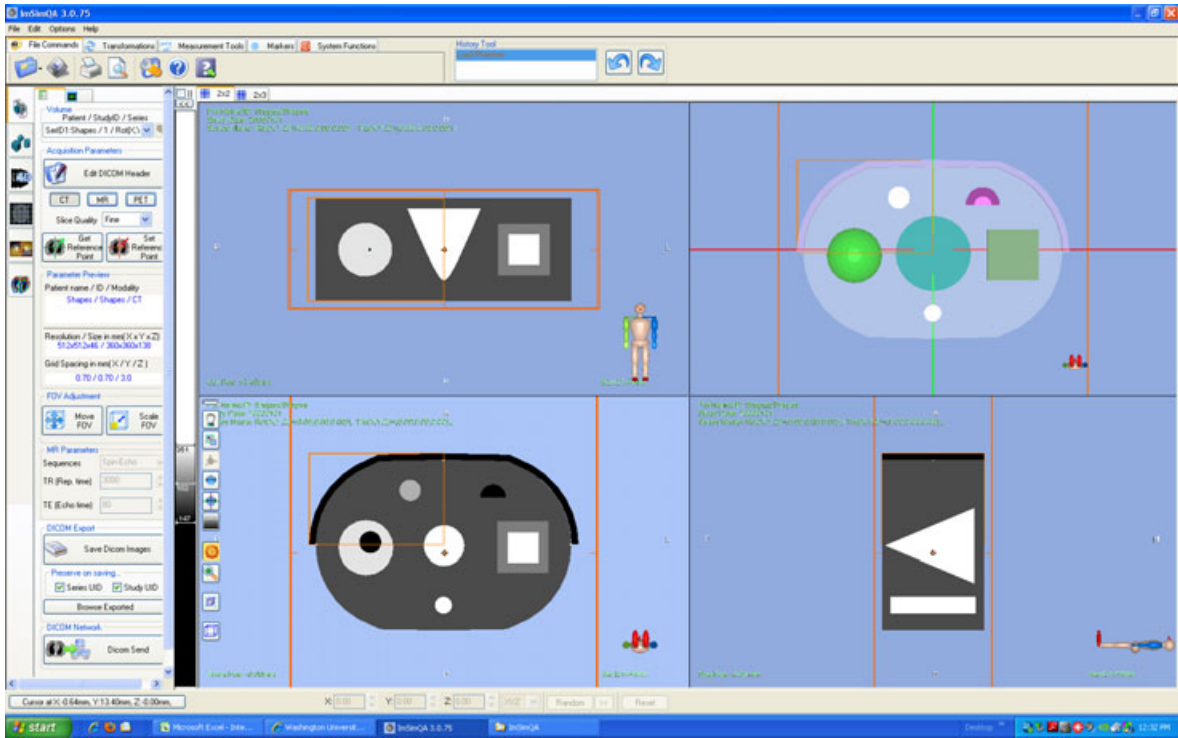
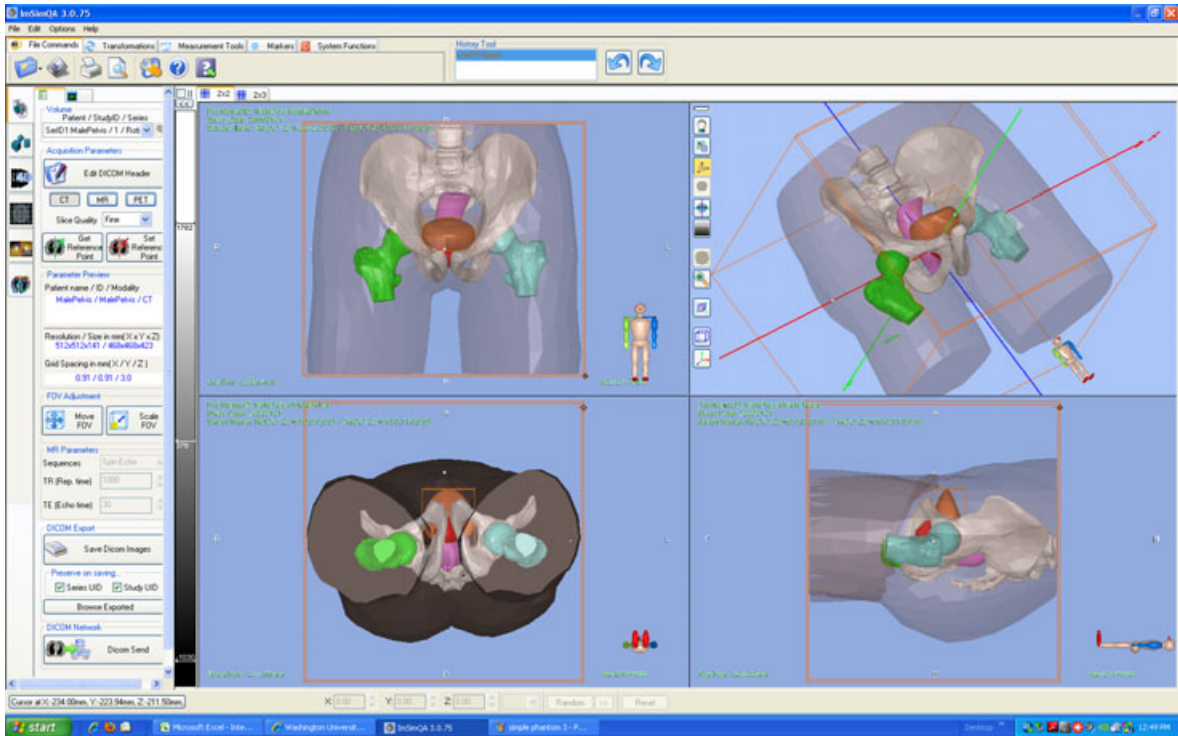**APPENDIX C: SCREENSHOTS OF PHANTOM DATASETS**

Figure C.1 Simple geometric CT Phantom

Figure C.2 Pelvis CT Phantom

VI.   REFERENCES

[1]J. Ashburner, "A fast diffeomorphic image registration algorithm," Neuroimage. **38**, 95-113 (2007).

[2]L. G. Brown, "A survey of image registration techniques," ACM computing surveys (CSUR). **24**, 325-376 (1992).

[3]A. Collignon, F. Maes, D. Delaere, D. Vandermeulen, P. Suetens, and G. Marchal, "Automated multi-modality image registration based on information theory," Information processing in medical imaging, **3**, 263-274. (1995).

[4]D. L. Hill, P. G. Batchelor, M. Holden, and D. J. Hawkes, "Medical image registration," Physics in medicine and biology. **46**, R1 (2001).

[5]M. Jenkinson, P. Bannister, M. Brady, and S. Smith, "Improved optimization for the robust and accurate linear registration and motion correction of brain images," Neuroimage. **17**, 825-841 (2002).

[6]F. Maes, D. Vandermeulen, and P. Suetens, "Comparative evaluation of multiresolution optimization strategies for multimodality image registration by maximization of mutual information," Medical image analysis. **3**, 373-386 (1999).

[7]B. Zitova and J. Flusser, "Image registration methods: a survey," Image and vision computing. **21**, 977-1000 (2003).

[8]J. A. Maintz and M. A. Viergever, "A survey of medical image registration," Medical image analysis. **2**, 1-36 (1998).

[9]M. van Herk, J. C. de Munck, J. V. Lebesque, S. Muller, C. Rasch, and A. Touw, "Automatic registration of pelvic computed tomography data and magnetic resonance scans including a full circle method for quantitative accuracy evaluation," Medical physics. **25**, 2054-2067 (1998).

[10]J. Cai, J. C. Chu, D. Recine, M. Sharma, C. Nguyen, R. Rodebaugh, V. A. Saxena, and A. Ali, "CT and PET lung image registration and fusion in radiotherapy treatment planning using the chamfer-matching method," International journal of radiation oncology, biology, physics. **43**, 883-891 (1999).

[11]M. Jobse, J. Davelaar, E. Hendriks, R. Kattevilder, H. Reiber, and B. Stoel, "A new algorithm for the registration of portal images to planning images in the verification of radiotherapy, as validated in prostate treatments," Medical physics. **30**, 2274-2281 (2003).

[12]M. van Herk and H. M. Kooy, "Automatic three-dimensional correlation of CT-CT, CT-MRI, and CT-SPECT using chamfer matching," Medical physics. **21**, 1163-1178 (1994).

[13]P. Papavasileiou, G. D. Flux, M. J. Guy, and M. A. Flower, "A novel four-dimensional image registration method for radionuclide therapy dosimetry," Phys Med Biol. **49**, 5373-5391 (2004).

[14]D. Sarrut, V. Boldea, S. Miguet, and C. Ginestet, "Simulation of four-dimensional CT images from deformable registration between inhale and exhale breath-hold CT scans," Medical physics. **33**, 605-617 (2006).

[15]R. Shekhar, P. Lei, C. R. Castro-Pareja, W. L. Plishker, and W. D. D'Souza, "Automatic segmentation of phase-correlated CT scans through nonrigid image registration using geometrically regularized free-form deformation," Medical physics. **34**, 3054-3066 (2007).

[16]T. Kunzler, J. Grezdo, J. Bogner, W. Birkfellner, and D. Georg, "Registration of DRRs and portal images for verification of stereotactic body radiotherapy: a feasibility study in lung cancer treatment," Phys Med Biol. **52**, 2157-2170 (2007).

[17]Y. Yin, E. A. Hoffman, and C. L. Lin, "Mass preserving nonrigid registration of CT lung images using cubic B-spline," Medical physics. **36**, 4213-4222 (2009).

[18]J. Moseley and P. Munro, "A semiautomatic method for registration of portal images," Medical physics. **21**, 551-558 (1994).

[19]A. Kano, K. Doi, H. MacMahon, D. D. Hassell, and M. L. Giger, "Digital image subtraction of temporally sequential chest images for detection of interval change," Medical physics. **21**, 453-461 (1994).

[20]L. Dong and A. L. Boyer, "An image correlation procedure for digitally reconstructed radiographs and electronic portal images," International journal of radiation oncology, biology, physics. **33**, 1053-1060 (1995).

[21]B. J. McParland and J. C. Kumaradas, "Digital portal image registration by sequential anatomical matchpoint and image correlations for real-time continuous field alignment verification," Medical physics. **22**, 1063-1075 (1995).

[22]A. A. Flynn, A. J. Green, G. Boxer, R. B. Pedley, and R. H. Begent, "A comparison of image registration techniques for the correlation of radiolabelled antibody distribution with tumour morphology," Phys Med Biol. **44**, N151-159 (1999).

[23]R. Tanaka, S. Sanada, M. Suzuki, T. Kobayashi, T. Matsui, H. Inoue, and N. Yoshihisa, "Breathing chest radiography using a dynamic flat-panel detector combined with computer analysis," Medical physics. **31**, 2254-2262 (2004).

[24]C. Studholme, D. L. Hill, and D. J. Hawkes, "Automated three-dimensional registration of magnetic resonance and positron emission tomography brain images by multiresolution optimization of voxel similarity measures," Med Phys. **24**, 25-35 (1997).

[25]T. Bruckner, R. Lucht, and G. Brix, "Comparison of rigid and elastic matching of dynamic magnetic resonance mammographic images by mutual information," Medical physics. **27**, 2456-2461 (2000).

[26]J. Kim, J. A. Fessler, K. L. Lam, J. M. Balter, and R. K. Ten Haken, "A feasibility study of mutual information based setup error estimation for radiotherapy," Medical physics. **28**, 2507-2517 (2001).

[27]B. M. Klabbers, J. C. de Munck, B. J. Slotman, H. A. Langendijk, R. de Bree, O. S. Hoekstra, R. Boellaard, and A. A. Lammertsma, "Matching PET and CT scans of the head and neck area: development of method and validation," Medical physics. **29**, 2230-2238 (2002).

[28]J. E. Bond, V. Smith, N. J. Yue, and J. P. Knisely, "Comparison of an image registration technique based on normalized mutual information with a standard method utilizing implanted markers in the

staged radiosurgical treatment of large arteriovenous malformations," International journal of radiation oncology, biology, physics. **57**, 1150-1158 (2003).

[29]S. Clippe, D. Sarrut, C. Malet, S. Miguet, C. Ginestet, and C. Carrie, "Patient setup error measurement using 3D intensity-based image registration techniques," International journal of radiation oncology, biology, physics. **56**, 259-265 (2003).

[30]N. Dekker, L. S. Ploeger, and M. van Herk, "Evaluation of cost functions for gray value matching of two-dimensional images in radiotherapy," Medical physics. **30**, 778-784 (2003).

[31]M. I. Miga, "A new approach to elastography using mutual information and finite elements," Phys Med Biol. **48**, 467-480 (2003).

[32]K. M. Brock, J. M. Balter, L. A. Dawson, M. L. Kessler, and C. R. Meyer, "Automated generation of a four-dimensional model of the liver using warping and mutual information," Medical physics. **30**, 1128-1133 (2003).

[33]X. Wu, S. J. Dibiase, R. Gullapalli, and C. X. Yu, "Deformable image registration for the use of magnetic resonance spectroscopy in prostate treatment planning," International journal of radiation oncology, biology, physics. **58**, 1577-1583 (2004).

[34]M. M. Coselmon, J. M. Balter, D. L. McShan, and M. L. Kessler, "Mutual information based CT registration of the lung at exhale and inhale breathing states using thin-plate splines," Med Phys. **31**, 2942-2948 (2004).

[35]W. C. Lavely, C. Scarfone, H. Cevikalp, R. Li, D. W. Byrne, A. J. Cmelak, B. Dawant, R. R. Price, D. E. Hallahan, and J. M. Fitzpatrick, "Phantom validation of coregistration of PET and CT for image-guided radiotherapy," Medical physics. **31**, 1083-1092 (2004).

[36]P. L. Roberson, P. W. McLaughlin, V. Narayana, S. Troyer, G. V. Hixson, and M. L. Kessler, "Use and uncertainties of mutual information for computed tomography/ magnetic resonance (CT/MR) registration post permanent implant of the prostate," Med Phys. **32**, 473-482 (2005).

[37]S. Ji, Z. Wu, A. Hartov, D. W. Roberts, and K. D. Paulsen, "Mutual-information-based image to patient re-registration using intraoperative ultrasound in image-guided neurosurgery," Medical physics. **35**, 4612-4624 (2008).

[38]S. Klein, U. A. van der Heide, I. M. Lips, M. van Vulpen, M. Staring, and J. P. Pluim, "Automatic segmentation of the prostate in 3D MR images by atlas matching using localized mutual information," Medical physics. **35**, 1407-1417 (2008).

[39]S. B. Park, F. C. Rhee, J. I. Monroe, and J. W. Sohn, "Spatially weighted mutual information image registration for image guided radiation therapy," Medical physics. **37**, 4590-4601 (2010).

[40]M. Marinelli, A. Martinez-Moller, B. Jensen, V. Positano, S. Weismuller, N. Navab, L. Landini, M. Schwaiger, and S. G. Nekolla, "Registration of myocardial PET and SPECT for viability assessment using mutual information," Medical physics. **37**, 2414-2424 (2010).

[41]J. Chappelow, B. N. Bloch, N. Rofsky, E. Genega, R. Lenkinski, W. DeWolf, and A. Madabhushi, "Elastic registration of multimodal prostate MRI and histology via multiattribute combined mutual information," Medical physics. **38**, 2005-2018 (2011).

[42]W. M. Wells, 3rd, P. Viola, H. Atsumi, S. Nakajima, and R. Kikinis, "Multi-modal volume registration by maximization of mutual information," Medical image analysis. **1**, 35-51 (1996).

[43]P. Viola and W. M. Wells III, "Alignment by maximization of mutual information," International journal of computer vision. **24**, 137-154 (1997).

[44]L. Hadjiiski, H. P. Chan, B. Sahiner, N. Petrick, and M. A. Helvie, "Automated registration of breast lesions in temporal pairs of mammograms for interval change analysis--local affine transformation for improved localization," Medical physics. **28**, 1070-1079 (2001).

[45]P. Filev, L. Hadjiiski, B. Sahiner, H. P. Chan, and M. A. Helvie, "Comparison of similarity measures for the task of template matching of masses on serial mammograms," Medical physics. **32**, 515-529 (2005).

[46]L. Xiong, A. Viswanathan, A. J. Stewart, S. Haker, C. M. Tempany, L. M. Chin, and R. A. Cormack, "Deformable structure registration of bladder through surface mapping," Medical physics. **33**, 1848-1856 (2006).

[47]J. Shi, B. Sahiner, H. P. Chan, L. Hadjiiski, C. Zhou, P. N. Cascade, N. Bogot, E. A. Kazerooni, Y. T. Wu, and J. Wei, "Pulmonary nodule registration in serial CT scans based on rib anatomy and nodule template matching," Medical physics. **34**, 1336-1347 (2007).

[48]F. Lamare, T. Cresson, J. Savean, C. Cheze Le Rest, A. J. Reader, and D. Visvikis, "Respiratory motion correction for PET oncology applications using affine transformation of list mode data," Phys Med Biol. **52**, 121-140 (2007).

[49]M. A. Jacobs, J. P. Windham, H. Soltanian-Zadeh, D. J. Peck, and R. A. Knight, "Registration and warping of magnetic resonance images to histological sections," Medical physics. **26**, 1568-1578 (1999).

[50]J. Lian, L. Xing, S. Hunjan, C. Dumoulin, J. Levin, A. Lo, R. Watkins, K. Rohling, R. Giaquinto, D. Kim, D. Spielman, and B. Daniel, "Mapping of the prostate in endorectal coil-based MRI/MRSI and CT: a deformable registration and validation study," Med Phys. **31**, 3087-3094 (2004).

[51]B. Schaly, J. A. Kempe, G. S. Bauman, J. J. Battista, and J. Van Dyk, "Tracking the dose distribution in radiation therapy by accounting for variable anatomy," Phys Med Biol. **49**, 791-805 (2004).

[52]M. Rosu, I. J. Chetty, J. M. Balter, M. L. Kessler, D. L. McShan, and R. K. Ten Haken, "Dose reconstruction in deforming lung anatomy: dose grid size effects and clinical implications," Medical physics. **32**, 2487-2495 (2005).

[53]N. Venugopal, B. McCurdy, A. Hnatov, and A. Dubey, "A feasibility study to investigate the use of thin-plate splines to account for prostate deformation," Phys Med Biol. **50**, 2871-2885 (2005).

[54]U. Malsch, C. Thieke, P. E. Huber, and R. Bendl, "An enhanced block matching algorithm for fast elastic registration in adaptive radiotherapy," Phys Med Biol. **51**, 4789-4806 (2006).

[55]H. Zhong, T. Peters, and J. V. Siebers, "FEM-based evaluation of deformable image registration for radiation therapy," Phys Med Biol. **52**, 4721-4738 (2007).

[56]Y. Xie, M. Chao, P. Lee, and L. Xing, "Feature-based rectal contour propagation from planning CT to cone beam CT," Medical physics. **35**, 4450-4459 (2008).

[57]Q. J. Wu, D. Thongphiew, Z. Wang, V. Chankong, and F. F. Yin, "The impact of respiratory motion and treatment technique on stereotactic body radiation therapy for liver cancer," Medical physics. **35**, 1440-1451 (2008).

[58]Y. Xie, M. Chao, and L. Xing, "Tissue feature-based and segmented deformable image registration for improved modeling of shear movement of lungs," International journal of radiation oncology, biology, physics. **74**, 1256-1265 (2009).

[59]J. Woo, P. J. Slomka, D. Dey, V. Y. Cheng, B. W. Hong, A. Ramesh, D. S. Berman, R. P. Karlsberg, C. C. Kuo, and G. Germano, "Geometric feature-based multimodal image registration of contrast-enhanced cardiac CT with gated myocardial perfusion SPECT," Medical physics. **36**, 5467-5479 (2009).

[60]G. Narayanasamy, G. L. LeCarpentier, M. Roubidoux, J. B. Fowlkes, A. F. Schott, and P. L. Carson, "Spatial registration of temporally separated whole breast 3D ultrasound images," Medical physics. **36**, 4288-4300 (2009).

[61]E. M. Vasquez Osorio, M. S. Hoogeman, L. Bondar, P. C. Levendag, and B. J. Heijmen, "A novel flexible framework with automatic feature correspondence optimization for nonrigid registration in radiotherapy," Medical physics. **36**, 2848-2859 (2009).

[62]L. Bondar, M. S. Hoogeman, E. M. Vasquez Osorio, and B. J. Heijmen, "A symmetric nonrigid registration method to handle large organ deformations in cervical cancer patients," Medical physics. **37**, 3760-3772 (2010).

[63]Y. Xie, M. Chao, and G. Xiong, "Deformable image registration of liver with consideration of lung sliding motion," Medical physics. **38**, 5351-5361 (2011).

[64]M. J. Pallone, P. M. Meaney, and K. D. Paulsen, "Surface scanning through a cylindrical tank of coupling fluid for clinical microwave breast imaging exams," Medical physics. **39**, 3102-3111 (2012).

[65]E. M. Vasquez Osorio, M. S. Hoogeman, A. Mendez Romero, P. Wielopolski, A. Zolnay, and B. J. Heijmen, "Accurate CTMR vessel-guided nonrigid registration of largely deformed livers," Medical physics. **39**, 2463-2477 (2012).

[66]S. Wognum, L. Bondar, A. G. Zolnay, X. Chai, M. C. Hulshof, M. S. Hoogeman, and A. Bel, "Control over structure-specific flexibility improves anatomical accuracy for point-based deformable registration in bladder cancer radiotherapy," Medical physics. **40**, 021702 (2013).

[67]I. Arganda-Carreras, C. O. Sorzano, P. Thevenaz, A. Munoz-Barrutia, J. Kybic, R. Marabini, J. M. Carazo, and C. Ortiz-de Solorzano, "Non-rigid consistent registration of 2D image sequences," Phys Med Biol. **55**, 6215-6242 (2010).

[68]W. Bai and M. Brady, "Regularized B-spline deformable registration for respiratory motion correction in PET images," Phys Med Biol. **54**, 2719-2736 (2009).

[69]J. Blumenfeld, C. Studholme, J. Carballido-Gamio, D. Carpenter, T. M. Link, and S. Majumdar, "Three-dimensional image registration of MR proximal femur images for the analysis of trabecular bone parameters," Medical physics. **35**, 4630-4639 (2008).

[70]M. Chao, J. Penagaricano, Y. Yan, E. G. Moros, P. Corry, and V. Ratanatharathorn, "Voxel-based dose reconstruction for total body irradiation with helical tomotherapy," International journal of radiation oncology, biology, physics. **82**, 1575-1583 (2012).

[71]A. R. Cunliffe, H. A. Al-Hallaq, Z. E. Labby, C. A. Pelizzari, C. Straus, W. F. Sensakovic, M. Ludwig, and S. G. Armato, "Lung texture in serial thoracic CT scans: assessment of change introduced by image registration," Medical physics. **39**, 4679-4690 (2012).

[72]V. Delmon, S. Rit, R. Pinho, and D. Sarrut, "Registration of sliding objects using direction dependent B-splines decomposition," Phys Med Biol. **58**, 1303-1314 (2013).

[73]E. Faggiano, C. Fiorino, E. Scalco, S. Broggi, M. Cattaneo, E. Maggiulli, I. Dell'Oca, N. Di Muzio, R. Calandrino, and G. Rizzo, "An automatic contour propagation method to follow parotid gland deformation during head-and-neck cancer tomotherapy," Phys Med Biol. **56**, 775-791 (2011).

[74]M. Hub, C. Thieke, M. L. Kessler, and C. P. Karger, "A stochastic approach to estimate the uncertainty of dose mapping caused by uncertainties in b-spline registration," Medical physics. **39**, 2186-2192 (2012).

[75]T. J. Jacobson and M. J. Murphy, "Optimized knot placement for B-splines in deformable image registration," Medical physics. **38**, 4579-4582 (2011).

[76]V. V. Karnik, A. Fenster, J. Bax, D. W. Cool, L. Gardi, I. Gyacskov, C. Romagnoli, and A. D. Ward, "Assessment of image registration accuracy in three-dimensional transrectal ultrasound guided prostate biopsy," Medical physics. **37**, 802-813 (2010).

[77]V. V. Karnik, A. Fenster, J. Bax, C. Romagnoli, and A. D. Ward, "Evaluation of intersession 3D-TRUS to 3D-TRUS image registration for repeat prostate biopsies," Medical physics. **38**, 1832-1843 (2011).

[78]S. Khallaghi, C. G. Leung, K. Hastrudi-Zaad, P. Foroughi, C. Nguan, and P. Abolmaesumi, "Experimental validation of an intrasubject elastic registration algorithm for dynamic-3D ultrasound images," Medical physics. **39**, 5488-5497 (2012).

[79]F. Lamare, M. J. Ledesma Carbayo, T. Cresson, G. Kontaxakis, A. Santos, C. C. Le Rest, A. J. Reader, and D. Visvikis, "List-mode-based reconstruction for respiratory motion correction in PET using non-rigid body transformations," Phys Med Biol. **52**, 5187-5204 (2007).

[80]S. Mori, T. Furukawa, T. Inaniwa, S. Zenklusen, M. Nakao, T. Shirai, and K. Noda, "Systematic evaluation of four-dimensional hybrid depth scanning for carbon-ion lung therapy," Medical physics. **40**, 031720 (2013).

[81]V. Pekar, E. Gladilin, and K. Rohr, "An adaptive irregular grid approach for 3D deformable image registration," Phys Med Biol. **51**, 361-377 (2006).

[82]Y. Petibon, J. Ouyang, X. Zhu, C. Huang, T. G. Reese, S. Y. Chun, Q. Li, and G. El Fakhri, "Cardiac motion compensation and resolution modeling in simultaneous PET-MR: a cardiac lesion detection study," Phys Med Biol. **58**, 2085-2102 (2013).

[83]E. Rietzel and G. T. Chen, "Deformable registration of 4D computed tomography data," Medical physics. **33**, 4423-4430 (2006).

[84]T. Rohlfing, C. R. Maurer, Jr., W. G. O'Dell, and J. Zhong, "Modeling liver motion and deformation during the respiratory cycle using intensity-based nonrigid registration of gated MR images," Medical physics. **31**, 427-432 (2004).

[85]E. Schreibmann, A. F. Waller, I. Crocker, W. Curran, and T. Fox, "Voxel clustering for quantifying PET-based treatment response assessment," Medical physics. **40**, 012401 (2013).

[86]E. Schreibmann and L. Xing, "Narrow band deformable registration of prostate magnetic resonance imaging, magnetic resonance spectroscopic imaging, and computed tomography studies," International journal of radiation oncology, biology, physics. **62**, 595-605 (2005).

[87]J. A. Shackleford, N. Kandasamy, and G. C. Sharp, "On developing B-spline registration algorithms for multi-core processors," Phys Med Biol. **55**, 6329-6351 (2010).

[88]N. Shusharina and G. Sharp, "Analytic regularization for landmark-based image registration," Phys Med Biol. **57**, 1477-1498 (2012).

[89]M. Staring, S. Klein, and J. P. Pluim, "A rigidity penalty term for nonrigid registration," Medical physics. **34**, 4098-4108 (2007).

[90]M. Staring, S. Klein, and J. P. Pluim, "Nonrigid registration with tissue-dependent filtering of the deformation field," Phys Med Biol. **52**, 6879-6892 (2007).

[91]Q. Tang, J. Cammin, S. Srivastava, and K. Taguchi, "A fully four-dimensional, iterative motion estimation and compensation method for cardiac CT," Medical physics. **39**, 4291-4305 (2012).

[92]C. Tanner, J. A. Schnabel, D. L. Hill, D. J. Hawkes, A. Degenhard, M. O. Leach, D. R. Hose, M. A. Hall-Craggs, and S. I. Usiskin, "Quantitative evaluation of free-form deformation registration for dynamic contrast-enhanced MR mammography," Medical physics. **34**, 1221-1233 (2007).

[93]R. W. van der Put, E. M. Kerkhof, B. W. Raaymakers, I. M. Jurgenliemk-Schulz, and J. J. Lagendijk, "Contour propagation in MRI-guided radiotherapy treatment of cervical cancer: the accuracy of rigid, non-rigid and semi-automatic registrations," Phys Med Biol. **54**, 7135-7150 (2009).

[94]J. Vandemeulebroucke, S. Rit, J. Kybic, P. Clarysse, and D. Sarrut, "Spatiotemporal motion estimation for respiratory-correlated imaging of the lungs," Medical physics. **38**, 166-178 (2011).

[95]P. C. Vos, T. Hambrock, J. O. Barenstz, and H. J. Huisman, "Computer-assisted analysis of peripheral zone prostate lesions using T2-weighted and dynamic contrast enhanced T1-weighted MRI," Phys Med Biol. **55**, 1719-1734 (2010).

[96]J. Wang and X. Gu, "High-quality four-dimensional cone-beam CT by deforming prior images," Phys Med Biol. **58**, 231-246 (2013).

[97]Z. Wu, E. Rietzel, V. Boldea, D. Sarrut, and G. C. Sharp, "Evaluation of deformable registration of patient lung 4DCT with subanatomical region segmentations," Medical physics. **35**, 775-781 (2008).

[98]G. Xiong, C. Chen, J. Chen, Y. Xie, and L. Xing, "Tracking the motion trajectories of junction structures in 4D CT images of the lung," Phys Med Biol. **57**, 4905-4930 (2012).

[99]C. Yan, H. Zhong, M. Murphy, E. Weiss, and J. V. Siebers, "A pseudoinverse deformation vector field generator and its applications," Medical physics. **37**, 1117-1128 (2010).

[100]C. Zhang, M. C. Villa-Uriol, M. De Craene, J. M. Pozo, J. M. Macho, and A. F. Frangi, "Dynamic estimation of three-dimensional cerebrovascular deformation from rotational angiography," Medical physics. **38**, 1294-1306 (2011).

[101]H. Zhong, J. Kim, and I. J. Chetty, "Analysis of deformable image registration accuracy using computational modeling," Medical physics. **37**, 970-979 (2010).

[102]H. Wang, L. Dong, J. O'Daniel, R. Mohan, A. S. Garden, K. K. Ang, D. A. Kuban, M. Bonnen, J. Y. Chang, and R. Cheung, "Validation of an accelerated 'demons' algorithm for deformable image registration in radiation therapy," Physics in medicine and biology. **50**, 2887-2905 (2005).

[103]A. L. Martel, M. S. Froh, K. K. Brock, D. B. Plewes, and D. C. Barber, "Evaluating an optical-flow-based registration algorithm for contrast-enhanced magnetic resonance imaging of the breast," Phys Med Biol. **52**, 3803-3816 (2007).

[104]D. Yang, H. Li, D. A. Low, J. O. Deasy, and I. El Naqa, "A fast inverse consistent deformable image registration method based on symmetric optical flow computation," Phys Med Biol. **53**, 6143-6165 (2008).

[105]R. Castillo, E. Castillo, R. Guerra, V. E. Johnson, T. McPhail, A. K. Garg, and T. Guerrero, "A framework for evaluation of deformable image registration spatial accuracy using large landmark point sets," Phys Med Biol. **54**, 1849-1870 (2009).

[106]E. Schreibmann, J. A. Nye, D. M. Schuster, D. R. Martin, J. Votaw, and T. Fox, "MR-based attenuation correction for hybrid PET-MR brain imaging systems using deformable image registration," Medical physics. **37**, 2101-2109 (2010).

[107]J. Ehrhardt, R. Werner, D. Saring, T. Frenzel, W. Lu, D. Low, and H. Handels, "An optical flow based method for improved reconstruction of 4D CT data sets acquired during free breathing," Medical physics. **34**, 711-721 (2007).

[108]J. W. Wolthaus, J. J. Sonke, M. van Herk, and E. M. Damen, "Reconstruction of a time-averaged midposition CT scan for radiotherapy planning of lung cancer patients using deformable registration," Medical physics. **35**, 3998-4011 (2008).

[109]X. Gu, B. Dong, J. Wang, J. Yordy, L. Mell, X. Jia, and S. B. Jiang, "A contour-guided deformable image registration algorithm for adaptive radiotherapy," Phys Med Biol. **58**, 1889-1901 (2013).

[110]J. Hou, M. Guerrero, W. Chen, and W. D. D'Souza, "Deformable planning CT to cone-beam CT image registration in head-and-neck cancer," Medical physics. **38**, 2088-2094 (2011).

[111]A. Bharatha, M. Hirose, N. Hata, S. K. Warfield, M. Ferrant, K. H. Zou, E. Suarez-Santana, J. Ruiz-Alzola, A. D'Amico, R. A. Cormack, R. Kikinis, F. A. Jolesz, and C. M. Tempany, "Evaluation of three-dimensional finite element-based deformable registration of pre- and intraoperative prostate imaging," Medical physics. **28**, 2551-2560 (2001).

[112]K. K. Brock, S. J. Hollister, L. A. Dawson, and J. M. Balter, "Technical note: creating a four-dimensional model of the liver using finite element analysis," Medical physics. **29**, 1403-1405 (2002).

[113]J. Liang and D. Yan, "Reducing uncertainties in volumetric image based deformable organ registration," Medical physics. **30**, 2116-2122 (2003).

[114]K. K. Brock, D. L. McShan, R. K. Ten Haken, S. J. Hollister, L. A. Dawson, and J. M. Balter, "Inclusion of organ deformation in dose calculations," Medical physics. **30**, 290-295 (2003).

[115]T. Zhang, N. P. Orton, T. R. Mackie, and B. R. Paliwal, "Technical note: A novel boundary condition using contact elements for finite element based deformable image registration," Medical physics. **31**, 2412-2415 (2004).

[116]K. K. Brock, M. B. Sharpe, L. A. Dawson, S. M. Kim, and D. A. Jaffray, "Accuracy of finite element model-based multi-organ deformable image registration," Medical physics. **32**, 1647-1659 (2005).

[117]K. K. Brock, L. A. Dawson, M. B. Sharpe, D. J. Moseley, and D. A. Jaffray, "Feasibility of a novel deformable image registration technique to facilitate classification, targeting, and monitoring of tumor and normal tissue," International journal of radiation oncology, biology, physics. **64**, 1245-1254 (2006).

[118]C. Tanner, J. A. Schnabel, D. L. Hill, D. J. Hawkes, M. O. Leach, and D. R. Hose, "Factors influencing the accuracy of biomechanical breast models," Medical physics. **33**, 1758-1769 (2006).

[119]R. Alterovitz, K. Goldberg, J. Pouliot, I. C. Hsu, Y. Kim, S. M. Noworolski, and J. Kurhanewicz, "Registration of MR prostate images with biomechanical modeling and nonlinear parameter estimation," Medical physics. **33**, 446-454 (2006).

[120]Y. Chi, J. Liang, and D. Yan, "A material sensitivity study on the accuracy of deformable organ registration using linear biomechanical models," Medical physics. **33**, 421-433 (2006).

[121]Q. Wu, J. Liang, and D. Yan, "Application of dose compensation in image-guided radiotherapy of prostate cancer," Phys Med Biol. **51**, 1405-1419 (2006).

[122]J. M. Hensel, C. Menard, P. W. Chung, M. F. Milosevic, A. Kirilova, J. L. Moseley, M. A. Haider, and K. K. Brock, "Development of multiorgan finite element-based prostate deformation model enabling registration of endorectal coil magnetic resonance imaging for radiotherapy planning," International journal of radiation oncology, biology, physics. **68**, 1522-1528 (2007).

[123]M. R. Kaus, K. K. Brock, V. Pekar, L. A. Dawson, A. M. Nichol, and D. A. Jaffray, "Assessment of a model-based deformable image registration approach for radiation therapy planning," International journal of radiation oncology, biology, physics. **68**, 572-580 (2007).

[124]A. M. Nichol, K. K. Brock, G. A. Lockwood, D. J. Moseley, T. Rosewall, P. R. Warde, C. N. Catton, and D. A. Jaffray, "A magnetic resonance imaging study of prostate deformation relative to implanted gold fiducial markers," International journal of radiation oncology, biology, physics. **67**, 48-56 (2007).

[125]K. K. Brock, A. M. Nichol, C. Menard, J. L. Moseley, P. R. Warde, C. N. Catton, and D. A. Jaffray, "Accuracy and sensitivity of finite element model-based deformable registration of the prostate," Medical physics. **35**, 4019-4025 (2008).

[126]A. Al-Mayah, J. Moseley, and K. K. Brock, "Contact surface and material nonlinearity modeling of human lungs," Phys Med Biol. **53**, 305-317 (2008).

[127]A. Al-Mayah, J. Moseley, M. Velec, and K. K. Brock, "Sliding characteristic and material compressibility of human lung: parametric study and verification," Medical physics. **36**, 4625-4633 (2009).

[128]T. N. Nguyen, J. L. Moseley, L. A. Dawson, D. A. Jaffray, and K. K. Brock, "Adapting liver motion models using a navigator channel technique," Medical physics. **36**, 1061-1073 (2009).

[129]A. Al-Mayah, J. Moseley, M. Velec, S. Hunter, and K. Brock, "Deformable image registration of heterogeneous human lung incorporating the bronchial tree," Medical physics. **37**, 4560-4571 (2010).

[130]A. Al-Mayah, J. Moseley, S. Hunter, M. Velec, L. Chau, S. Breen, and K. Brock, "Biomechanical-based image registration for head and neck radiation treatment," Phys Med Biol. **55**, 6491-6500 (2010).

[131]O. Alonzo-Proulx, N. Packard, J. M. Boone, A. Al-Mayah, K. K. Brock, S. Z. Shen, and M. J. Yaffe, "Validation of a method for measuring the volumetric breast density from digital mammograms," Phys Med Biol. **55**, 3027-3044 (2010).

[132]C. L. Eccles, L. A. Dawson, J. L. Moseley, and K. K. Brock, "Interfraction liver shape variability and impact on GTV position during liver stereotactic radiotherapy using abdominal compression," International journal of radiation oncology, biology, physics. **80**, 938-946 (2011).

[133]A. Al-Mayah, J. Moseley, M. Velec, and K. Brock, "Toward efficient biomechanical-based deformable image registration of lungs for image-guided radiotherapy," Phys Med Biol. **56**, 4701-4713 (2011).

[134]H. Zhong, J. Kim, H. Li, T. Nurushev, B. Movsas, and I. J. Chetty, "A finite element method to correct deformable image registration errors in low-contrast regions," Phys Med Biol. **57**, 3499-3515 (2012).

[135]L. Han, J. H. Hipwell, C. Tanner, Z. Taylor, T. Mertzanidou, J. Cardoso, S. Ourselin, and D. J. Hawkes, "Development of patient-specific biomechanical models for predicting large breast deformation," Phys Med Biol. **57**, 455-472 (2012).

[136]D. N. Levin, C. A. Pelizzari, G. Chen, C. Chen, and M. Cooper, "Retrospective geometric correlation of MR, CT, and PET images," Radiology. **169**, 817-823 (1988).

[137]D. L. Hill, D. J. Hawkes, and C. R. Hardingham, "Use of anatomical knowledge to register 3-D blood vessel data derived from DSA with MR images," Medical Imaging V: Image Processing, 348-357. (1991).

[138]W. R. Fright and A. D. Linney, "Registration of 3-D head surfaces using multiple landmarks," IEEE Transactions on medical imaging. **12**, 515-520 (1993).

[139]K. Gilhuijs and M. Van Herk, "Automatic on-line inspection of patient setup in radiation therapy using digital portal images," Medical physics. **20**, 667-677 (1993).

[140]D. L. Hill, D. J. Hawkes, N. A. Harrison, and C. F. Ruff, "A strategy for automated multimodality image registration incorporating anatomical knowledge and imager characteristics," Biennial International Conference on Information Processing in Medical Imaging, 182-196. (1993).

[141]P. Hua and I. Fram, "Feature-based image registration for digital subtraction angiography," Medical Imaging 1993, 24-31. (1993).

[142]M. I. Miller, G. E. Christensen, Y. Amit, and U. Grenander, "Mathematical textbook of deformable neuroanatomies," Proceedings of the National Academy of Sciences. **90**, 11944-11948 (1993).

[143]G. Striano and F. Fazio, "A procedure for patient repositioning and compensation for misalignment between transmission and emission data in PET heart studies," (1993).

[144]P. A. Van den Elsen, E.-J. Pol, and M. A. Viergever, "Medical image matching-a review with classification," IEEE Engineering in Medicine and Biology Magazine. **12**, 26-39 (1993).

[145]R. P. Woods, J. C. Mazziotta, and S. R. Cherry, "MRI-PET registration with automated algorithm," Journal of computer assisted tomography. **17**, 536-546 (1993).

[146]A. Liu, S. M. Pizer, D. H. Eberly, B. S. Morse, J. G. Rosenman, E. L. Chaney, E. Bullitt, and V. Carrasco, "Volume registration using the 3D core," Visualization in Biomedical Computing 1994, 217-226. (1994).

[147]N. Kirby, C. Chuang, and J. Pouliot, "A two-dimensional deformable phantom for quantitatively verifying deformation algorithms," Medical physics. **38**, 4583-4586 (2011).

[148]T. Juang, S. Das, J. Adamovics, R. Benning, and M. Oldham, "On the need for comprehensive validation of deformable image registration, investigated with a novel 3-dimensional deformable dosimeter," International journal of radiation oncology, biology, physics. **87**, 414-421 (2013).

[149]H. N. Christiansen and T. W. Sederberg, "Conversion of complex contour line definitions into polygonal element mosaics," ACM Siggraph Computer Graphics, **12**, 187-192. (1978).

[150]K. K. Brock, "Imaging and image-guided radiation therapy in liver cancer," Seminars in radiation oncology. **21**, 247-255 (2011).

[151]M. J. Murphy, "Image-guided patient positioning: if one cannot correct for rotational offsets in external-beam radiotherapy setup, how should rotational offsets be managed?," Medical physics. **34**, 1880-1883 (2007).

[152]E. A. Eisenhauer, P. Therasse, J. Bogaerts, L. H. Schwartz, D. Sargent, R. Ford, J. Dancey, S. Arbuck, S. Gwyther, M. Mooney, L. Rubinstein, L. Shankar, L. Dodd, R. Kaplan, D. Lacombe, and J. Verweij, "New response evaluation criteria in solid tumours: Revised RECIST guideline (version 1.1)," European Journal of Cancer. **45**, 228-247 (2009).

[153]A. M. Badawi, E. Weiss, W. C. Sleeman, and G. D. Hugo, "Classifying geometric variability by dominant eigenmodes of deformation in regressing tumours during active breath hold lung cancer radiotherapy," Physics in medicine and biology. **57**, 395-413 (2012).

[154]S. Rit, H. J. Kuijf, S. van Kranen, M. van Herk, and J.-J. Sonke, "Computer assisted analysis of lung tumor regression during radiotherapy."

[155]M. L. Kessler, "Image registration and data fusion in radiation therapy," The British journal of radiology. **79 Spec No 1**, S99-108 (2006).

[156]L. E. Court, L. Dong, N. Taylor, M. Ballo, K. Kitamura, A. K. Lee, J. O'Daniel, R. A. White, R. Cheung, and D. Kuban, "Evaluation of a contour-alignment technique for CT-guided prostate radiotherapy: an intra- and interobserver study," International Journal of Radiation Oncology • Biology • Physics. **59**, 412-418

[157]K. M. Langen, Y. Zhang, R. D. Andrews, M. E. Hurley, S. L. Meeks, D. O. Poole, T. R. Willoughby, and P. A. Kupelian, "Initial experience with megavoltage (MV) CT guidance for daily prostate alignments," International Journal of Radiation Oncology*Biology*Physics. **62**, 1517-1524 (2005).

[158]J. M. Fitzpatrick, J. B. West, and C. R. Maurer, Jr., "Predicting error in rigid-body point-based registration," IEEE Trans Med Imaging. **17**, 694-702 (1998).

[159]G. F. Persson, D. E. Nygaard, C. Hollensen, P. Munck af Rosenschold, L. S. Mouritsen, A. K. Due, A. K. Berthelsen, J. Nyman, E. Markova, A. P. Roed, H. Roed, S. Korreman, and L. Specht, "Interobserver delineation variation in lung tumour stereotactic body radiotherapy," Br J Radiol. **85**, e654-660 (2012).

[160]C. L. Brouwer, R. J. Steenbakkers, E. van den Heuvel, J. C. Duppen, A. Navran, H. P. Bijl, O. Chouvalova, F. R. Burlage, H. Meertens, J. A. Langendijk, and A. A. van 't Veld, "3D Variation in delineation of head and neck organs at risk," Radiation oncology. **7**, 32 (2012).

[161]B. E. Nelms, W. A. Tome, G. Robinson, and J. Wheeler, "Variations in the contouring of organs at risk: test case from a patient with oropharyngeal cancer," International journal of radiation oncology, biology, physics. **82**, 368-378 (2012).

[162]L. R. Dice, "Measures of the Amount of Ecologic Association Between Species," Ecology. **26**, 297-302 (1945).

[163]V. K. Chalana, Yongmin, "A Methodology for Evaluation of Boundary Detection Algorithms on Medical Images," IEEE Transactions on Medical Imaging. **16**, 642-652 (1997).

[164]W. P. Segars, B. M. Tsui, D. S. Lalush, E. C. Frey, M. A. king, and D. Manocha, "Development and application of the new dynamic Nurbs-based Cardiac-Torso (NCAT) phantom," Journal of Nuclear Medicine. **42**, (2001).

[165]R. Kashani, M. Hub, M. L. Kessler, and J. M. Balter, "Technical note: a physical phantom for assessment of accuracy of deformable alignment algorithms," Medical physics. **34**, 2785-2788 (2007).

[166]M. Serban, E. Heath, G. Stroian, D. L. Collins, and J. Seuntjens, "A deformable phantom for 4D radiotherapy verification: design and image registration evaluation," Medical physics. **35**, 1094-1102 (2008).

[167]Y. Y. Vinogradskiy, P. Balter, D. S. Followill, P. E. Alvarez, R. A. White, and G. Starkschall, "Comparing the accuracy of four-dimensional photon dose calculations with three-dimensional calculations using moving and deforming phantoms," Medical physics. **36**, 5000-5006 (2009).

[168]J. P. Bissonnette, P. A. Balter, L. Dong, K. M. Langen, D. M. Lovelock, M. Miften, D. J. Moseley, J. Pouliot, J. J. Sonke, and S. Yoo, "Quality assurance for image-guided radiation therapy utilizing CT-based technologies: a report of the AAPM TG-179," Medical physics. **39**, 1946-1963 (2012).

[169]B. Fraass, K. Doppke, M. Hunt, G. Kutcher, G. Starkschall, R. Stern, and J. Van Dyke, "American Association of Physicists in Medicine Radiation Therapy Committee Task Group 53: quality assurance for clinical radiotherapy treatment planning," Medical physics. **25**, 1773-1829 (1998).

[170]I. A. E. Agency, "Commissioning and Quality Assurance of Computerized Planning Systems for Radiation Treatment of Cancer," (International Atomic Energy Agency, Vienna, 2004), pp. 281.

[171]R. Castillo, E. Castillo, R. Guerra, V. E. Johnson, T. McPhail, A. K. Garg, and T. Guerrero, "A framework for evaluation of deformable image registration spatial accuracy using large landmark point sets," Physics in medicine and biology. **54**, 1849 (2009).

[172]R. Kashani, M. Hub, J. M. Balter, M. L. Kessler, L. Dong, L. Zhang, L. Xing, Y. Xie, D. Hawkes, and J. A. Schnabel, "Objective assessment of deformable image registration in radiotherapy: A multi-institution study," Medical physics. **35**, 5944-5953 (2008).

[173]J. Vandemeulebroucke, S. Rit, J. Kybic, P. Clarysse, and D. Sarrut, "Spatiotemporal motion estimation for respiratory-correlated imaging of the lungs," Medical physics. **38**, 166-178 (2011).

[174]K. K. Brock and D. R. A. Consortium, "Results of a multi-institution deformable registration accuracy study (MIDRAS)," International Journal of Radiation Oncology* Biology* Physics. **76**, 583-596 (2010).

[175]L. Potters, B. Kavanagh, J. M. Galvin, J. M. Hevezi, N. A. Janjan, D. A. Larson, M. P. Mehta, S. Ryu, M. Steinberg, R. Timmerman, J. S. Welsh, S. A. Rosenthal, R. American Society for Therapeutic, Oncology, and R. American College of, "American Society for Therapeutic Radiology and Oncology (ASTRO) and American College of Radiology (ACR) practice guideline for the performance of stereotactic body radiation therapy," International journal of radiation oncology, biology, physics. **76**, 326-332 (2010).